Journal of Building Engineering 127 (2026) 116361

Contents lists available at ScienceDirect

Journal of Building Engineering

journal homepage: www.elsevier.com/locate/jobe

A validated model for short-term prediction of cooling energy consumption in buildings - first step to forecast control of cooling

Wiktoria Łokczewska [a,*], Tomasz Cholewa [a], Amelia Staszowska [a], Constantinos A. Balaras [b], Paris A. Fokaides [c,d], Chirag Deb [e], Gerardo Maria Mauro [f], Fabrizio Ascione [g]

[a] Faculty of Environmental Engineering and Energy, Lublin University of Technology, Nadbystrzycka 40B, 20-618, Lublin, Poland
[b] Institute for Environmental Research & Sustainable Development, National, Observatory of Athens, I. Metaxa & Vas. Pavlou, GR-15236, Athens, Greece
[c] School of Engineering, Frederick University, 7, Frederickou Str., 1036, Nicosia, Cyprus
[d] Faculty of Civil Engineering and Architecture, Kaunas University of Technology, Lithuania
[e] School of Architecture, Design and Planning, The University of Sydney, Darlington, NSW, 2008, Australia
[f] Department of Architecture, Università degli Studi di Napoli Federico II, Via Forno Vecchio 36, 80134, Napoli, Italy
[g] Department of Industrial Engineering, Università degli Studi di Napoli Federico II, Piazzale Tecchio 80, 80125, Napoli, Italy

ARTICLE INFO

Keywords:
Buildings
Energy consumption
Modelling
Forecast control of cooling
Outdoor impacts

ABSTRACT

Smart control of energy supply for cooling in buildings can significantly improve energy efficiency. However, existing modelling methods are often complex and rely mainly on artificial neural networks (ANN) and other machine learning techniques, posing various difficulties for integrating them in forecast control of cooling. Moreover, accurate cooling energy models are generally more demanding to develop than heating models. To address this research gap, this study proposes a novel, simple and physically based method for creating building cooling energy models that also take into account the characteristics of the existing cooling system. The approach uses measured cooling energy consumption and meteorological data-outdoor air temperature, wind speed and solar irradiance - to derive an equivalent outdoor temperature that represents the real thermal behaviour of the building during cooling operation. Proper selection of operating and weather data is essential to minimise the influence of unrelated factors. The method is demonstrated on an office building in Poland and a university building in Cyprus. For both case studies, the developed cooling energy models were validated, achieving for outdoor temperatures above 26 °C mean absolute percentage error (MAPE) values of 13.15% for the office building and 17.87% for the university building. To further assess robustness, Multilayer Perceptron (MLP) ANN models were trained using the same hourly inputs-outdoor temperature, wind speed and solar radiation. The ANN models did not significantly improve prediction accuracy, yielding higher MAPE values of 19.6–24.7% for the office building and 29.4–34.9% for the university building. The results highlight that buildings must be considered individually and show that the proposed method can provide a practical, transparent and accurate tool for estimating cooling energy performance. Future work will address occupant influence and integration into predictive control of air-conditioning systems.

* Corresponding author.
E-mail address: s99258@pollub.edu.pl (W. Łokczewska).

https://doi.org/10.1016/j.jobe.2026.116361
Received 2 January 2026; Received in revised form 15 March 2026; Accepted 18 May 2026
Available online 20 May 2026

Nomenclature:

Abbreviations:

AC – Air Conditioning
ANN – Artificial Neural Network
CEHT – Cumulative Effect of High Temperature
CNN – Convolutional Neural Network
CV – Coefficient of Variation
CVRMSE – Coefficient of Variation of the Root Mean Square Error
DNN – Deep Neural Network
HVAC – Heating, Ventilation, Air Conditioning
LSTM – Long Short-Term Memory
MAE – Mean Absolute Error
MAPE – Mean Absolute Percentage Error
MLR – Multiple Linear Regression
MPC – Model Predictive Control
PET – Physiological Equivalent Temperature
RMSE – Root Mean Square Error
SOS – Sum-of-squares error function
TRN – Transformer neural network
VRF – Variable Refrigerant Flow
WAPE – Weighted Absolute Percentage Error

Symbols

E_C – hourly cooling energy consumption [kWh]
I_{nsol} – solar irradiance [W/m^2]
R^2 – Coefficient of Determination
T_{insol}^{rev} – outdoor temperature correction due to solar irradiance [°C]
$T_{outdoor}$, T_{out} – outdoor temperature [°C]
$T_{outdoor}^{eq}$, T_{eq} – equivalent outdoor temperature [°C]
T_{wind}^{rev} – outdoor temperature correction due to wind speed [°C]
V_{mean} – mean wind speed [m/s]

1. Introduction

In 2023, the global energy demand in buildings surpassed 120 EJ, representing 28% of total final energy consumption, while from 2010 to 2023, the energy demand in buildings grew at a mean annual rate of 0.9% [1]. The United States, the European Union, and China were responsible for nearly half of global energy consumption in buildings.

Since 2010, the global building floor area has increased by over 31%, exceeding 250 billion square meters, with nearly 80% of this space accounted for by residential buildings [2]. This growth has contributed to an energy demand increase, with the building sector experiencing an annual increase of over 1%. Electricity consumption in buildings increased from 30% in 2010 to 35% in 2022 [3], largely driven by the growing demand for space cooling.

The rapid growth in global air conditioning demand is placing an unprecedented strain on electricity grids worldwide. In the hottest regions of the world cooling can account for over 70% of peak electricity demand [4] [5]. Improving the energy efficiency of air conditioning technologies and implementing demand response strategies are critical for reducing electricity consumption, mitigating greenhouse gas (GHG) emissions, and ensuring the stability of power systems during periods of high power demand [4].

Climate change is driving an increase in global temperatures, leading to a growing demand for cooling not only in traditionally hot regions, but also in the areas that have not previously experienced high temperatures and cooling loads. Furthermore, improving living standards and higher demand for indoor thermal comfort are further fuelling the demand for the use of air conditioning in buildings [6]. According to the United Nations Representative Concentration Pathways (RCP) scenarios, global temperatures are projected to rise substantially, especially under RCP8.5. This increase in temperature will directly lead to a higher number of cooling degree days and thus elevate the energy demand for air conditioning. Moreover, income growth remains the dominant driver of air conditioner adoption, with temperature influencing operational usage intensity [7].

In particular, space cooling remains the fastest-growing energy demand in the building sector [8]. Projections indicate that, under the Stated Policies Scenario (STEPS), the global demand for space cooling in buildings will grow at a mean annual rate of 3.7% until 2035, with over 90% of this increase occurring in emerging markets and developing economies [9]. This is attributed to economic growth, rising incomes, and a warming climate, which in turn intensifies cooling needs and increases system workload. As the demand for cooling is rising, it increases the overall electrical energy consumption and also contributes to higher peak electricity loads, placing additional pressure on the power grids.

Heat waves further accelerate this trend, significantly boosting air conditioning use and sales.

More frequent and intense heat waves could increase electricity demand for cooling by as much as 20% above current projections, with the majority of this increase concentrated in developing

regions [9].

To lower the rapid increase in electricity demand for cooling and the growing strain on power grids, the emphasis has been placed on improving the efficiency of air conditioning systems. On the other hand, traditional cooling strategies, which rely on reactive or rule-based controls, often fail to optimize energy consumption effectively. To address this challenge, predictive methods are being developed, leveraging advanced modelling techniques and real-time data to enhance system efficiency.

Several studies have adopted classical machine learning techniques such as decision trees, artificial neural networks, ensemble methods, linear regression, and boosting algorithms for cooling energy prediction. These approaches represent the foundation of data-driven modelling in building energy research, offering interpretable yet efficient alternatives to physics-based models. However, their performance strongly depends on data availability, feature selection, and the level of model generalization.

Numerous studies have explored energy consumption forecasting for cooling, utilizing machine learning, artificial intelligence, and neural networks to improve predictive accuracy (see Table 1). These advanced computational approaches have demonstrated significant potential in optimising cooling system performance.

The reviewed studies show that the most frequently applied approaches fall into two broad categories: regression-based simplified physical models and data-driven machine learning techniques. Regression methods-particularly multivariable linear regression (MLR) and its extensions-are widely used because of their transparency, low data requirements, and ease of calibration.

These models often rely on meteorological drivers. Nonlinear regression (MNR) further improves accuracy by capturing dynamic and nonlinear interactions, while interval estimation methods add robustness by quantifying predictive uncertainty.

In contrast, data-driven approaches-such as artificial neural networks (ANN), support vector regression (SVR), gradient boosting (XGBoost), and recurrent neural networks (LSTM, GRU)-consistently achieve strong predictive accuracy, particularly for short-term horizons. Their strength lies in capturing complex patterns directly from operational data. However, they typically require large, high-quality datasets and suffer from limited interpretability. Hybrid and decomposition-based models attempt to bridge this gap by combining physical interpretability with advanced data-driven learning.

Against this backdrop, the equivalent outdoor temperature (T_{eq}) method proposed in this paper distinguishes itself by remaining in the category of simplified physical models, but explicitly enhancing the external driver through corrections for solar irradiance and wind speed adjusted to specific buildings and their air conditioning system. Unlike conventional degree-day or temperature-only regressions, this approach embeds key atmospheric factors into a single explanatory variable, improving a realistic physical representation without the need to use complex machine learning processes. As a result, the T_{eq}-based model provides a practical middle ground: interpretable, computationally efficient, and less data-intensive, while still addressing a known weakness of traditional regression approaches-the omission of critical meteorological corrections. Table 2 presents a comparison of different methods applied for forecasting cooling energy demand, highlighting their underlying approach, prediction accuracy, and associated error metrics.

The development of real energy models for existing buildings remains an unresolved issue, with no fully developed methodology available to date. These models are needed to estimate the separate and actual impact of each external environmental parameter - such as wind speed, solar radiation and outdoor temperature - on the building's energy demand for space cooling. The impact of external factors is not clearly emphasised in the current processes used to develop these types of energy performance models for buildings, which limits the ability to create forecasting models enabling their subsequent integration into predictive control strategies for cooling systems.

In addition, the process of creating energy models for cooling demand prediction is more complex in comparison to energy models for heating. That is why, developing such approaches could provide a more accessible and practical alternative, particularly for

Table 1
Overview of published approaches to building energy modelling for cooling purposes and associated data sources.

Authors	Type of proposed method	Type of analysed data
Borowski and Zwolińska, 2020 [10] [11]	Machine Learning	Measured Data
Feng et al., 2021 [12]	Machine Learning	Measured Data
Amasyali et al., 2021 [13]	Machine Learning	EnergyPlus simulations
Feng et al., 2022 [14]	Machine Learning	Measured Data
Khorrami et al., 2024 [15]	Machine Learning	ML data mining repository
Zhou et al., 2024 [16]	Machine Learning	Measured Data
Ascione et al., 2023 [17]	MPC, multi-objective genetic algorithm	Simulated Data and Measured Data
Yue et al., 2023 [18]	Selecting similar days methods	Measured Data
Li et al., 2023 [19]	TRN	Measured Data
Lu et al., 2023 [20]	LSTM	Measured Data
Zhao et al., 2023 [21]	LSTM	Measured Data
Chen et al., 2024 [22]	CNN	Measured Data
Vergés et al., 2024 [23]	ANN	Measured Data
Huang et al., 2024 [24]	LSTM	Measured Data
Song et al., 2024 [25]	LSTM	Measured Data
Park et al., 2025 [26]	LSTM	Measured Data
Aruta et al., 2025 [27]	ANN	Simulated Data
Hsu et al., 2025 [28]	LSTM	Measured Data

Table 2
Comparison of different methods applied for forecasting cooling energy demand, highlighting their underlying approach, prediction accuracy, and associated error metrics.

Study	Method (core idea)	Model class	Horizon/data	Reported accuracy
Guo et al. (2015) [29],	Improved Multivariable Linear Regression (MLR) with Principal Component Analysis (PCA), Cumulative Effect of High Temperature (CEHT), and dynamic two-step correction	Simplified physical (regression)	Daily mean cooling load, office buildings	Mean absolute relative error <8%
Chen et al. (2022) [30],	Physics-based Multivariable Linear Regression (MLR) with online calibration; drivers include temperature, relative humidity (RH), wind speed (WS), and solar radiation	Simplified physical (grey-box)	Hourly, building-level	Best Mean Absolute Percentage Error (MAPE) = 2.64%; Coefficient of Variation of the Root Mean Square Error (CVRMSE) ≤30% acceptable
Fan & Ding (2019) [31],	Multiple Nonlinear Regression (MNR) with sensitivity-based variable selection and calibration	Nonlinear regression	Hourly, large public buildings	Improved accuracy compared with MLR and Autoregressive with Exogenous inputs (ARX); higher robustness to dynamic changes
Zhang et al. (2017) [32],	Error correction + prediction interval estimation with MLR and Support Vector Regression (SVR); feature selection via distance correlation	Regression + uncertainty quantification	Hourly, EnergyPlus-simulated office	Accuracy improved after correction; reliable Prediction Interval Coverage Probability (PICP)
Lin et al. (2019) [33],	Load Component Disaggregation (LCD) via sparse coding into conduction, solar, fresh air, and internal gains; sub-load forecasting with Backpropagation Neural Network (BP-NN) and AutoRegressive Integrated Moving Average (ARIMA)	Data-driven (component-based)	Hourly, civilian building (Tianjin)	Higher accuracy than conventional data-driven models; interpretable sub-loads
Fan, Xiao & Zhao (2017) [34],	Deep autoencoder feature extraction + Extreme Gradient Boosting (XGBoost)	Data-driven	24-h ahead, building-level	CVRMSE ≈ 22.8%; linear baselines >30%
Yu et al. (2023) [35],	Comparison of XGBoost, Long Short-Term Memory (LSTM), Gated Recurrent Unit (GRU) recurrent neural networks, and Attention-based LSTM (A-LSTM)	Data-driven	1-h and 24-h ahead, district energy system	1-h ahead: CVRMSE ≈ 14.5% (XGBoost); 24-h ahead: best A-LSTM CVRMSE ≈ 26.6%
Feng et al. (2025) [36],	Hybrid surrogate with load disaggregation; combines simplified physical structure with machine learning (ML)	Hybrid	Daily profiles including demand response	Coefficient of Determination (R^2) > 0.98, CVRMSE <0.13; up to R^2 > 0.99, CVRMSE <0.11; ~760× faster than EnergyPlus simulation
Łokczewska et al. (this study)	Equivalent Outdoor Temperature (T_{eq}) with corrections for wind speed and solar irradiance	Simplified physical (T_{eq} model)	Hourly, two public buildings	Office Building - MAPE ≈ 13.15 %, CVRMSE ≈ 16.59 %, University Building - MAPE ≈ 17.87 %, CVRMSE ≈ 22.36 %,

applications where complex data-driven models are not feasible or necessary.

The concept of the Equivalent Outdoor Temperature (T_{eq}) is used to integrate multiple environmental influences-such as air temperature, solar radiation, sky radiation, humidity, and wind into a single parameter that more realistically represents the thermal impact of outdoor conditions on buildings. This makes it a popular method that is used for studies of cooling demand and thermal performance.

Recent research has shown that T_{eq} is particularly valuable when traditional approaches based only on air temperature are insufficient. For example, Jay et al. [37] introduced T_{eq} into co-heating and co-cooling test methods, extending their applicability to sunnier and warmer climates. By including radiative effects, T_{eq} reduces the problems that are associated with the collinearity between solar gains and outdoor temperature, thus enabling more accurate estimates of the Heat Transfer Coefficient (HTC) during the summer periods [37]. In building cooling load calculations, approaches such as the Total Equivalent Temperature Difference (TETD) method are closely related to the T_{eq} concept. Omar et al. [38] demonstrated that TETD can be applied effectively under hot climate conditions, incorporating both external and internal loads (ventilation, solar gains through walls, windows, roofs, etc.) to predict HVAC requirements with simplified calculation tools [38]. Cholewa et al. [39] further highlighted the relevance of T_{eq} in the building sector by experimentally estimating factors influencing T_{eq} in multifamily buildings, pointing out its usefulness for evaluating energy efficiency strategies and envelope performance. Although not identical, studies on Physiological Equivalent Temperature (PET) also revealed the importance of "equivalent" metrics that combine multiple climatic parameters into one index [40]. PET is mainly applied to human thermal comfort outdoors, while T_{eq} is typically applied to building performance and cooling energy estimation [40].

Overall, the literature indicates that T_{eq} and related methods provide a more comprehensive framework for modelling cooling demand, especially in climates where solar radiation and other environmental factors strongly influence the building indoor conditions. However, the existing methods on the equivalent outdoor temperature are generally static, not adjusted to specific buildings and the characteristics of the installed air conditioning system, while they also require large amounts of input data. In contrast, the novel energy model presented in this work introduces an innovative, building-specific approach for deriving a building energy model that is tailored to the building and the installed air conditioning system, and significantly reduces the necessary input data requirements,

while providing tailored results for the analysed building.

Similarly, there are many available methods and demanding simulation tools for the forecast of energy consumption for cooling but there is a noticeable gap in availability of simple, widely applicable methods. Particularly, there is limited research concerning simplified methods that rely on the physical dependencies and thermal behaviour of buildings that operate in the cooling mode under specific conditions and may be easily integrated in forecast control of cooling. Relevant work has been developed for forecast control of heating systems [39,41,42], leading to significant energy savings. However, similar solutions for cooling systems are still limited. Accurate short-term cooling demand forecasts are particularly useful for building managers and energy service companies, as they enable more efficient operation and form a key input for forecast-based cooling control. By allowing cooling systems to anticipate future cooling loads rather than operate reactively, such approaches have the potential to reduce energy use and peak demand. The main challenge remains to optimize the energy use by use of widely applicable forecast control of the cooling system while ensuring thermal comfort conditions for the occupants. This is not easy to achieve due to the strong and complex dependency of cooling energy demand on dynamic weather conditions, solar load, thermal resistance and inertia of the building envelope, and the dynamic performance of the cooling systems. This work aims to bridge this gap by proposing a universal method that enables, for each analysed building, the consideration of these interdependencies, thereby allowing a realistic representation of the building's thermal behaviour during the cooling mode and creating the possibility of its integration in forecast control of the cooling system.

Based on this, this work contributes to the advancement of research in the domain of building energy models for cooling by presenting a universally applicable, accurate, and automated approach with minimal complexity for the development of energy models based on the concept of an equivalent outdoor temperature (T_{eq}). The proposed approach distinctly accounts for the individual impacts of external factors, namely wind speed, solar radiation and outdoor temperature, on the buildings energy characteristic and the cooling system performance. In this context, the primary objective of the present work is to systematically investigate the energy characteristics of buildings and their cooling systems. The proposed methodology enables the formulation of a generalized, accurate, and automated modelling framework that can be implemented in diverse building types.

Section 2 outlines the characteristics of the buildings selected for the analysis. Section 3 provides a detailed, stepwise description of the methodological framework. Section 4 presents the results obtained during the validation phase and offers a comprehensive discussion regarding the method's performance and applicability. Section 5 summarizes the main findings of this study, highlights the contributions of the proposed methodology, and discusses potential directions for future research.

2. Input data - case studies

The input data used to develop the building energy models for cooling were collected from two public utility buildings (Fig. 1) equipped with VRF air conditioning systems (summarized in Table 3).

Building A is located in Łódź (central Poland) that is characterized as a moderate climate zone with cooling degree days (CDD) of 39.10 and heating degree days of 769.48 in 2024 (source: Eurostat). It is a historic, post-industrial structure that underwent extensive modernisation and now serves as an office building. It is situated in the city centre and consists of two parts: the main 5-story building and a 4-story annex. It offers a total area of 5000 m^2. The building is equipped with seven VRF-type air conditioning systems featuring cassette-type indoor units. The interior air conditioned spaces are designated for office, conference, and social functions, including shared areas such as a kitchen and dining room. The basic technical parameters of the cooling system for Building A are presented in Table 3.

The building is equipped with a mechanical ventilation system, and a VRF air conditioning system that is managed with individual controls located in each room. The electrical energy consumption data for the operation of the VRF system in the entire building were collected on an hourly basis for two cooling seasons during 2022 (01.05.2022-30.09.2022) and 2023 (01.05.2023-31.08.2023). Outdoor weather data were also collected for the same periods for the specific location of the analysed building, namely: $T_{outdoor}$ -

Fig. 1. Overview of the analysed buildings: Building A (office) and building B (educational).

Table 3
Characteristics of the cooling systems in Building A and Building B.

Building	Type	Number of floors	Number of VRF Systems	Cooling Power (Total Cooling Capacity) [kW]	Total air conditioned area [m^2]	Type of indoor units
A	Office	5	7	413 kW	3814.3 m^2	cassette-type indoor units
B	Educational	3	1	285 kW	1101 m^2	cassette-type indoor units

outdoor temperature [°C], V_{mean} – mean wind speed [m/s], I_{nsol} – total solar irradiance on the horizontal [W/m^2] and RH – relative humidity [%]. An overview of the collected data is summarized in Table 4.

Building B is an educational facility located in Nicosia, Cyprus. The building is equipped with a central VRF cooling system serving a total air-conditioned area of 1101 m^2 across three storeys. The cooling capacity is approximately equally distributed among the three floors. Each floor is divided into separate functional zones. The system consists of 4-way ceiling-mounted cassette indoor units controlled individually in each room and a central VRF inverter system with five outdoor units. The basic technical parameters of the cooling system for Building B are presented in Table 3. The ground floor houses a cafeteria, the first floor contains three seminar rooms, while the second floor accommodates office spaces and a conference room. Given that the cooling season largely coincides with the vacation period of the students resulting in limited use of the common areas, the analysis was restricted for this building to the office and conference spaces located on the **second floor** to ensure data relevance and consistency with occupancy patterns. Only the second floor, with an area of approximately 367 m^2, is considered in the energy model development process. This approach minimises variability due to differing usage profiles across building zones, enhancing the reliability of the study findings. Additionally, a weather station located near the campus measures outdoor weather conditions at 30-min intervals including outdoor temperature ($T_{outdoor}$ in [°C]), humidity (RH in [%]), mean wind speed (V_{mean} in [m/s]), and total solar irradiance on the horizontal (I_{nsol} in [W/m^2]). The characteristics of the instrumentation used during the monitoring campaign are summarized in Table 4.

The building is located on the campus of Frederick University, in a region characterized by a Mediterranean climate, which is defined by hot and dry summers with CDD in 2024 of 1010.96 and HDD of 510.14 in 2024 for Cyprus (source: Eurostat). The comparison of the Degree Days for the two locations in Poland and Cyprus over the period 2022–2024 is presented in Table 5.

The data collected for this building cover the entire period of 2023 and 2024, but for the analysis in this work, only the data corresponding to the period from 01.05.2023 to 31.09.2023 and 01.05.2024 – 30.08.2024 were considered. The energy consumption data for the operation of the VRF system on the second floor in this building were collected in 30-min intervals and integrated on an hourly basis for the two cooling seasons in 2023 and 2024.

For both buildings analysed in this study, the datasets were collected from their respective VRF type air-conditioning monitoring systems. Measurements were recorded from both outdoor and indoor units, capturing operational states and energy consumption.

3. Method

This section presents a new method that estimates the influence of external factors, such as outdoor temperature ($T_{outdoor}$), solar irradiance (I_{nsol}) and wind speed (V_{mean}) on energy consumption for space cooling (see Fig. 2) that may be then used for the forecast control of cooling systems. Utilizing the meteorological conditions facilitates the calculation of an actual energy model of the building for cooling purposes that is based on physical dependencies. In the frame of this research, the indoor relative humidity (RH) was also measured. However, for the analysed buildings there was no significant influence on the energy consumption for cooling since the resulting correlation was 0.1477 for Building A and 0.2624 for Building B. Although the impact of RH was not integrated in this study, it is recommended to check its potential influence on energy consumption for cooling of a specific building during future studies that may lead to include it since it depends on the characteristics of the specific cooling systems and local weather conditions.

The developed universal calculation algorithm allows for the consideration of the actual operating conditions of the cooling system that is related to an equivalent outdoor temperature, which reflects the contribution of both wind speed and solar irradiance by using

Table 4
Accuracy of sensors used for measurements of outdoor conditions.

Location	Parameter	Accuracy
Nicosia, Cyprus	Outdoor Temperature [°C]	±0.21 °C from 0° to 50 °C
	RH [%]	±2.5% from 10% to 90% RH typical to a maximum of ±3.5% including hysteresis at 25 °C; below 10% and above 90% ± 5% typical
	Wind Speed [m/s]	±1.1 m/s or ±5% of reading
	Solar irradiance [W/m^2]	±10 W/m^2 or ±5%
Łódź, Poland	Outdoor Temperature [°C]	±0.3 °C
	RH [%]	±1.0%
	Wind Speed [m/s]	±0.5 m/s
	Solar irradiance [W/m^2]	±20 W/m^2

Table 5
Comparison of heating degree days (HDD) and cooling degree days (CDD) for Łódź and Cyprus in 2022–2024 [43].

Location	HDD[a] [°C·day]			CDD[b] [°C·day]		
	2022	2023	2024	2022	2023	2024
City of Łódź	3275	3005	2769	27	18	39
Cyprus	696	530	510	698	780	1011

[a] HDD (Heating Degree Days): base temperature = 18 °C.
[b] CDD (Cooling Degree Days): base temperature = 21 °C.

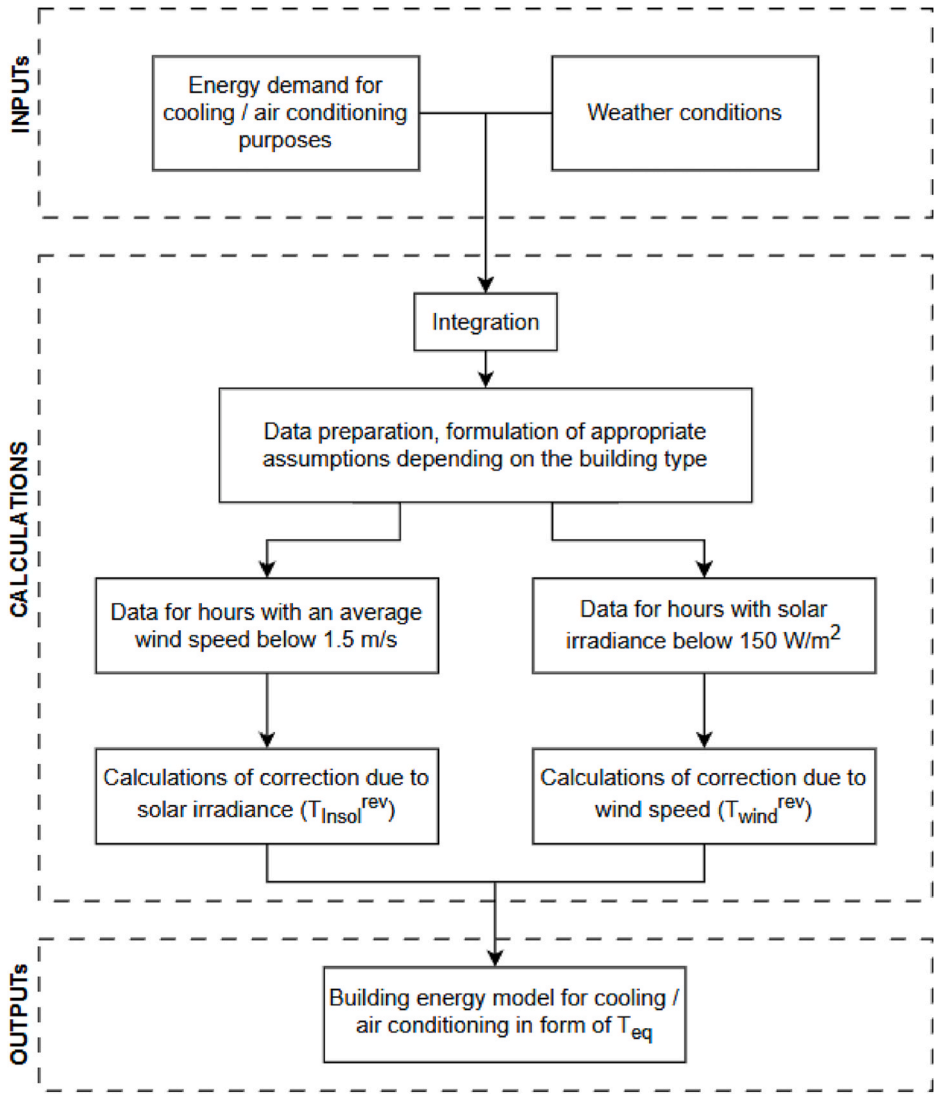

Fig. 2. The methodology of creating a simple building energy model for cooling in a form of equivalent outdoor temperature.

corrections (T_{wind}^{rev}, T_{Insol}^{rev}) of the outdoor temperature (see equations (1.1)-(1.3)). Finally, this approach enables the calculation of the energy demand for space cooling by taking into account the impact of the outdoor weather conditions on the cooling system energy demand.

$$T_{outdoor}{}^{eq} = T_{outdoor} - T_{wind}{}^{rev} + T_{insol}{}^{rev} \tag{1.1}$$

$$T_{wind}{}^{rev} = a_v \cdot V_{mean} + b_v \tag{1.2}$$

$$T_{insol}{}^{rev} = a_i \cdot I_{nsol} + b_i \tag{1.3}$$

where:

a_v – slope coefficient of the function that defines the correction of the outdoor temperature due to wind speed [−];

b_v – y-intercept of the function that defines the correction of the outdoor temperature due to wind speed [−];

a_i – slope coefficient of the function that defines the correction of the outdoor temperature due to solar irradiance [−];

b_i – y-intercept of the function that defines the correction of the outdoor temperature due to solar irradiance [−].

The effect of wind speed on the reduction of heat transfer is linked through the influence of the convective heat transfer mechanisms, since the convective heat transfer coefficient h is strongly dependent on air velocity near the surface (Newton's law of cooling: $qconv = h \cdot \Delta T$). Lower wind speeds reduce the convective heat removal rate, thus increasing the surface temperatures. Similarly, solar irradiance directly contributes to the radiative heat gains through absorption, which can be approximated by $q_{rad} = \alpha I_{nsol}$ where α is the absorptivity and I_{nsol} the incident solar flux. These physical principles provide the basis for the applied linear correction forms, which represent first-order approximations of the underlying transfer processes. While simplified, they capture the dominant trends and ensure practical applicability of the model. The relationships between cooling energy consumption and the considered variables were approximated using linear functions to ensure model simplicity and interpretability. Additionally, the linear formulation allows straightforward corrections for external factors such as solar irradiance and wind speed, which would be more complex to implement in nonlinear models.

The details of the process of estimation of outdoor temperature corrections due to solar irradiance and wind speed are presented in sections 3.1-3.2.

3.1. Selection of measured data for cooling energy analysis

In the process of preparing the input data for the follow up analysis, it is essential to appropriately select measurements that reflect the typical operational conditions of a given building type. In most cases, air conditioning systems operate only when people are present in the conditioned spaces and actively use them. The presence and activity of users directly influence when the system is activated, the duration of its operation, and the intensity of its use. This corresponds to the individualized control of the system, achieved through room-mounted controllers within the air-conditioned spaces. Such a control strategy is implemented in both buildings considered in this analysis. Consequently, it is crucial to exclude the time periods in which the cooling system is not functioning or operating at minimal levels (standby mode) in a specific building.

Including data from periods that the building or some zones and spaces are not occupied and the VRF system is not in operation, can disrupt the accurate determination of relationships between outdoor weather conditions and cooling energy consumption. For example, weekend weather conditions may feature high outdoor temperature and intense solar radiation, yet energy consumption for cooling during these periods is minimal since the building will be unoccupied leading to reduced operational demand on the cooling system.

To ensure the integrity of the analysis, the data related to energy consumption for cooling purposes in the analysed buildings (building A and building B) were carefully filtered to correspond to the occupancy periods (see Table 6). The observations corresponding to weekends, holidays, and hours outside the standard working schedule-defined as 7:00-16:00 for the analysed office building (building A) and 10:00-20:00 for the analysed university facilities (building B)-were excluded.

These periods were determined following a detailed review of both the measurement data and the operational characteristics of the buildings. During the excluded periods, the use of interior spaces is significantly reduced, and the air conditioning systems have minimal operation with very low cooling energy consumption, if any. To ensure the reliability of the analysis, only data reflecting cooling energy consumption above the minimum power required for air conditioning system standby operation mode were included. The baselines were established by averaging the measured hourly electrical energy use by the VRF systems during the standby periods resulting to a value of 0.3 kWh for Building A and 0.4 kWh for Building B. The standby energy was estimated using the mean night time electricity consumption, during which periods the air conditioning system was known to be inactive and the measured energy use corresponded solely to the essential power needed to keep the system on standby (for Building A, the value was calculated as the mean

Table 6
Main data selection assumptions for the two analysed buildings.

Parameters	Assumptions for the Office Building (Building A)	Assumptions for the University Building (Building B)
Analysed Time Period for Training	Two cooling seasons 01.05.2022-31.09.2022 01.05.2023-30.08.2023	Two cooling seasons 01.05.2023-31.09.2023 01.05.2024-30.08.2024
Analysed Days of the Week	Monday to Friday	Monday to Friday
Analysed Working Hours	7:00 a.m. – 4:00 p.m.	10:00 a.m. – 8:00 p.m.
Minimum Hourly Cooling Energy Consumption Required for System Standby	0.3 kWh	0.4 kWh
Public Holidays	Weekends and public holidays were excluded from the data base used in the analysis	Weekends and public holidays were excluded from the data base used in the analysis
Validation period	1 month – September 2023	1 month – September 2024

for all seven VRF systems in the building). Energy consumption values in each building below the corresponding baseline were considered non-representative of actual system operation and thus excluded from the dataset. Including very low energy consumption values could introduce distortions in the derived performance characteristics, particularly in relation to the outdoor weather conditions. For example, on a day with high outdoor temperatures, the system might have been inactive due to maintenance or user intervention, resulting in an unrealistic very low cooling energy consumption. Such cases may obscure the true relationship between cooling demand and external climatic factors. During periods with reduced cooling loads, energy consumption is often influenced by variables unrelated to the prevailing outdoor weather conditions and is connected directly with the standby mode.

Thus, excluding the non-occupancy periods from the analysis, it becomes possible to model and visualise the relationships between energy consumption for cooling and weather variables with greater accuracy (see Figs. 3 and 4).

On the basis of the data presented in Figs. 3 and 4 it is evident that it is crucial to properly screen the available data for achieving accurate model fitting. In the case of building A, which is an office building, the initial model, before the selection of relevant data, exhibited a correlation coefficient (R^2) of 0.4086. However, after the appropriate selection and incorporation of data (described before) that accurately reflects the building's cooling system operation, the R^2 value significantly improved to 0.6573. Similarly, for building B, an educational facility, the baseline model, which was developed without data selection, yielded a correlation coefficient of 0.5408. After implementing a careful selection of data relevant to the building's cooling performance, the R^2 value increased to 0.6852.

For Building A, a polynomial function was also tested, yielding coefficients of determination of 0.5409 for the full dataset and 0.7332 for the screened data. However, in order to maintain methodological simplicity and clarity, a linear function was chosen as the representative model.

The assumptions for other buildings should generally be defined in accordance with the building's typology and its operational characteristics. It is not possible to clearly differentiate residential and non-residential buildings, as both their operation and the performance of their air-conditioning systems may vary on a case-by-case basis. However, when selecting the appropriate assumptions, the guidelines presented in Table 7 can be used as a reference.

In many cases, air conditioning systems are switched on only during specific hours of the day and on certain days of the week. For example, for office-type buildings typically the cooling system is operating during typical working days and working hours, which is what was observed in the case of analysed buildings. The identification and selection of these operational periods must therefore be tailored to the building type. By carefully selecting the data corresponding to actual cooling operation times, the resulting energy model more accurately reflects the real performance of the air conditioning system, leading to significantly improved model fitting and predictive capability.

3.2. *Calculation of outdoor temperature corrections considering external parameters*

Solar radiation is a crucial influencing parameter affecting the intensity of solar heat gains of a building and consequently has a major impact on cooling energy consumption. The extent of solar heat gains is determined mainly by the building's architecture like window to wall ratio, orientation, shading devices, neighbouring obstacles, among others. As a result, there are varying levels of solar heat gains for different buildings under identical horizontal solar irradiance conditions.

Additionally, high wind speeds increase convective heat transfer and heat dissipation through the exposed walls, windows or other external surfaces. This is particularly important in the case of buildings with a large external surface or limited thermal insulation. It also contributes to a rise in negative pressure within natural or mechanical ventilation systems, potentially enhancing outdoor air

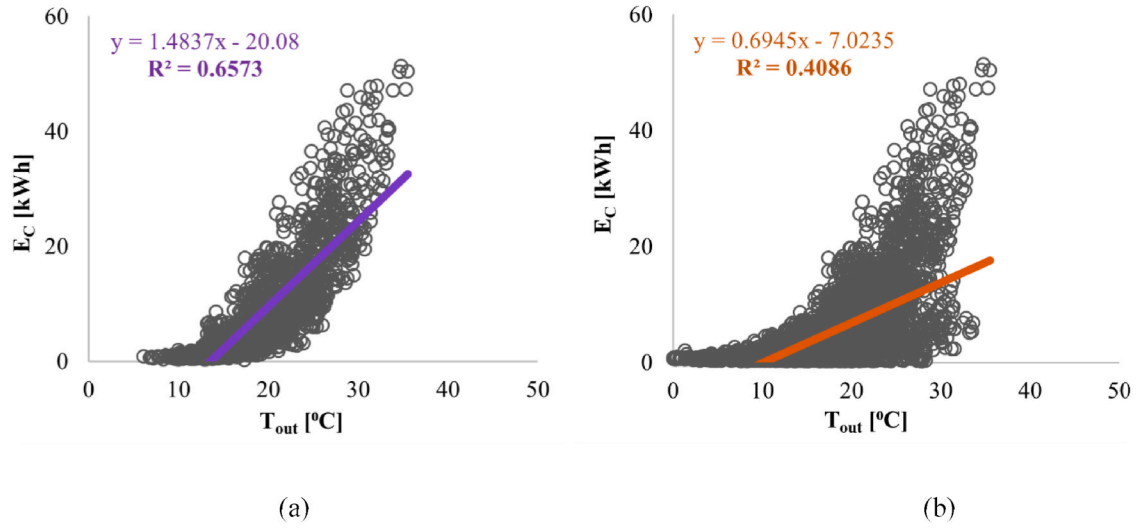

Fig. 3. Hourly cooling energy consumption (E_C) in Building A depending on the outdoor temperature T_{out}. (a) comparison before (with all measured data) and (b) comparison after (with screened data for occupancy periods), considering data selection assumptions.

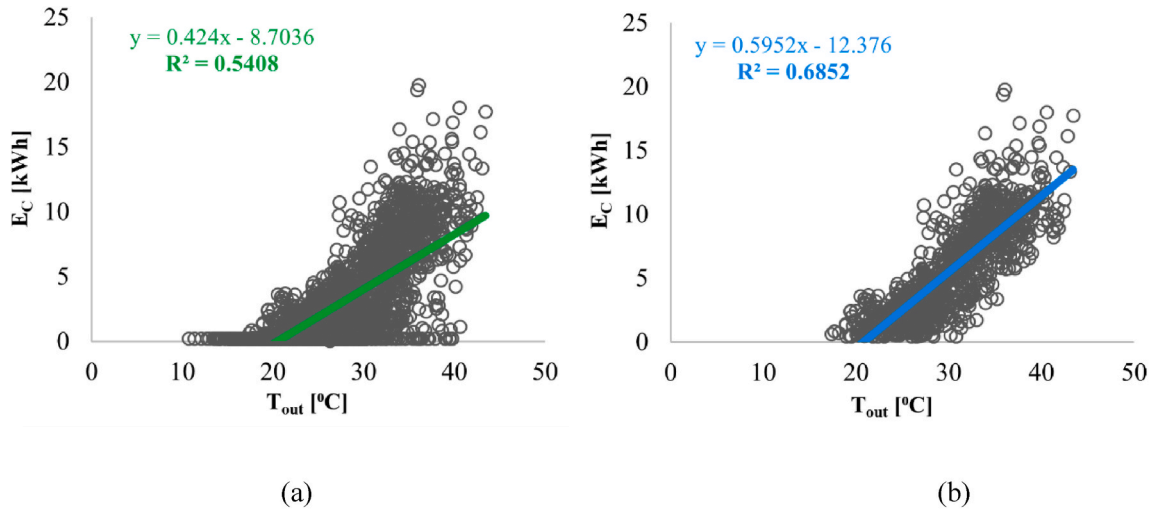

Fig. 4. Hourly cooling energy consumption (E_C) in Building B depending on the outdoor temperature T_{out} (a) comparison before (left with all measured data) and (b) comparison after (with screened data for occupancy periods) considering data selection assumptions.

Table 7
General assumptions and guidelines for data filtering in energy consumption databases for air-conditioning, supporting model development for buildings.

Parameters	Proposed Assumptions
Analysed Time Period for Training	Minimum 3 month (summer period).
Analysed Days of the Week	Depending on building typology: – **Residential, hotels** (buildings with continuous occupancy) – all week. – **Non-residential buildings** (e.g. Offices, Public Offices, Malls, Schools, Restaurants, Conference Centers) – working days.
Analysed Working Hours	Depending on working/using hours – **Residential buildings**, the periods of highest occupancy typically occur in the afternoon and evening hours during weekdays, as well as throughout the weekends from morning until evening. – **Non-residential buildings** follow their operating hours, with offices and schools used mainly 7 a.m.–5 PM, restaurants and malls from 8 a.m. to 9 PM, and hotels for 24 h a day.
Minimum Hourly Cooling Energy Consumption Required for System Standby	Mean value for night hours and hours when the AC is not working.
Public Holidays	Weekends and public holidays should be excluded from the data base used in the analysis – only for non-residential buildings that are not operating during holidays.
Validation period	Minimum 1 month.

infiltration and increasing the overall air exchange rate. As a result high wind speed can reduce the energy demand for space cooling in tight buildings with mechanical ventilation. However, it should be noted that an increased wind speed does not always reduce cooling loads, as higher infiltration under hot outdoor conditions can lead to a greater cooling load. The impact of wind direction is also important, with northern winds typically associated with lower outdoor temperatures, while southern winds usually result to higher outdoor temperatures that increase cooling demand. However, the analysis in this paper considers buildings with mechanical ventilation only.

Considering these factors is essential for building an energy model for cooling, as they significantly influence heat gains and losses in a building, and affect the overall energy consumption. The corrections for both these factors are determined using a similar approach, with the primary differences arising from the assumptions made for the values across different ranges. To describe the methodology, only the detailed calculation of the correction due to solar irradiance will be presented; for wind speed correction, only the differences that need to be considered during the calculations will be indicated.

While developing the equation to adjust outdoor temperature based on solar irradiance it is necessary to define the data range for which the impact of other influencing factors (such as high wind speed) is minimised. Therefore, only the data points where wind speed was less than 1.5 m/s were used for the correction calculations. The 1.5 m/s threshold was selected based on the specific dataset available for this building and location. Wind speed thresholds should be determined individually, depending on the measured data for each building and site, as local wind conditions vary significantly. The selected value should represent relatively low wind speeds that are typical for the given location. In general, a threshold of around 1.5 ± 1 m/s can be considered a safe and representative value for categorising low wind speed ranges in similar analyses. For the wind speed correction calculations, the dataset included only values where solar irradiance was below 150 W/m^2. This generally corresponds to early morning, late afternoon, or periods with high outdoor

temperature and large cloud cover – periods when buildings may have limited occupancy and cooling demand. Furthermore, this approach was intended to minimise the impact of solar gains and better isolate the effect of wind speed on equivalent outdoor temperature. If the dataset does not contain a sufficient number of data points below 150 W/m^2 for the analysis, it is also acceptable to use data with a mean solar irradiance below 200 W/m^2 or even up to 250 W/m^2 to ensure adequate sample size, while still limiting the variability introduced by solar radiation. This allows for extracting an appropriate dataset for which the impact of high wind speeds or high solar irradiance is minimised, enabling a more accurate estimation of the correction. The use of histograms can be helpful in the process of building a dataset for correction calculations.

The obtained dataset was then divided into several subsets based on the intensity of the external factors. If there are data points that disrupt the logical sequence of the dataset, they can be considered erroneous measurements and rejected during the model development process. For example, measurements that deviate significantly from the majority of data points can simply be considered gross errors and excluded from the analyses. The selection of the ranges depends on the available data and should be determined individually after analysing the solar irradiance levels and wind speeds at the building's location and assessing how the building responds to this external factor. It is best to analyse the available data to identify the minimum and maximum values and then divide the range into at least three approximately equal intervals of solar irradiance and wind speeds.

Fig. 5 illustrates the dependence of energy consumption for cooling on outdoor temperature for different solar irradiance ranges in dataset where wind speed was below 1.5 m/s for Building A.

The relationship between cooling energy consumption and outdoor temperature was determined using a simple linear regression and defining the coefficient of determination (R^2). Subsequently, using the determined linear regression equations, the cooling energy consumption was calculated for outdoor temperatures in the range of +24 °C to +40 °C (Table 8). Furthermore, for each building, a set of results is selected that logically represents the dependencies: as the outdoor temperature increases, the cooling energy consumption also increases; additionally, as solar irradiance increases, the cooling energy consumption also increases (for wind speed correction - also an appropriate dataset should be selected, reflecting that with increasing wind speed, cooling energy consumption decreases). In addition, analysis revealed that a logical trend where higher solar irradiance corresponds to higher energy consumption for cooling became evident when the outdoor air temperature exceeded 26 °C (see Table 8), as indicated by increased cooling energy demand above this threshold, which is also commonly adopted in thermal comfort and cooling load standards. Observed (Fig. 5) energy consumption above the standby level at temperatures below 26 °C results from partial operation of the system in selected spaces, rather than full-load operation throughout the building. This partial-load behaviour is strongly influenced by occupant activity, which is not explicitly accounted for in the current study. For the purpose of isolating the influence of external factors, the periods when the user's impact is minimised were selected, ensuring logical dependencies between cooling energy consumption and external conditions. Although energy consumption above standby is observed below 26 °C, the system is not operating at full capacity in most spaces. In future work, it is planned to address this aspect by introducing user behavior profiles to better account for internal influences on cooling energy demand. The red colored fonts and shaded area identify the logical scope of data taken for further analysis in case of solar irradiance and building A.

Following the selection of appropriate values for further analysis, the initial correction value (k_{sol_i}) of the outdoor temperature due to solar irradiance was determined (Table 9) by use of equations 2.1-2.3. This correction accounts for the temperature increase, ensuring that the regression equation with a lower equivalent solar irradiance yields the same cooling power as the higher solar

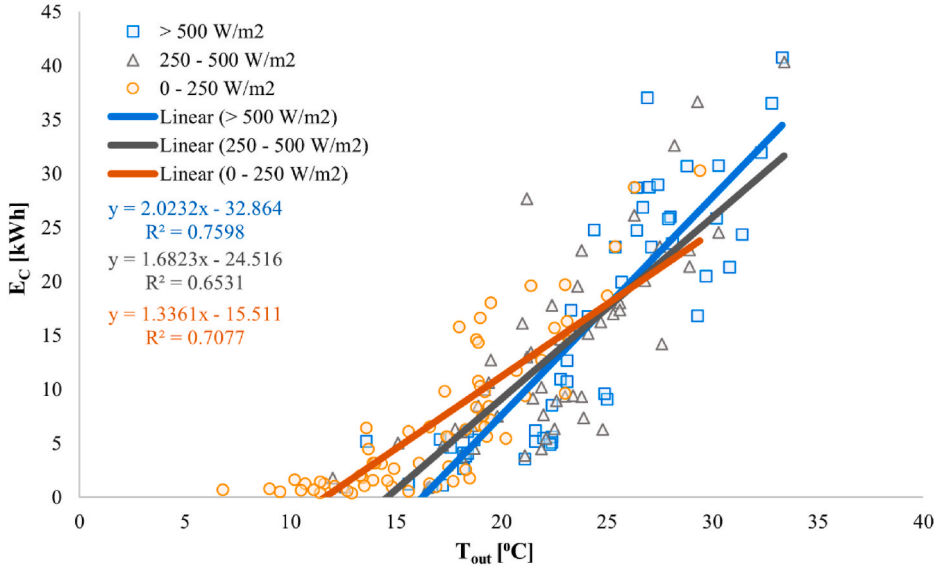

Fig. 5. Dependence of hourly cooling energy consumption on outdoor temperature for different solar irradiance ranges in dataset where wind speed was below 1.5 m/s for Building A.

Table 8
Summary of energy consumption for air conditioning in kWh calculated using the developed linear regression equations for specific solar irradiance ranges and a given outdoor temperature for Building A.

	Solar irradiance [W/m^2]		
	0-250	250-500	>500
T_{out} [°C]	(eq_1) y = 1.3361x - 15.511	(eq_2) y = 1.6823x - 24.516	(eq_3) y = 2.0232x - 32.864
24	16.555	15.859	15.693
25	17.892	17.542	17.716
26	19.228	19.224	19.739
27	**20.564**	**20.906**	**21.762**
28	**21.900**	**22.588**	**23.786**
29	**23.236**	**24.271**	**25.809**
30	**24.572**	**25.953**	**27.832**
31	**25.908**	**27.635**	**29.855**
32	**27.244**	**29.318**	**31.878**
33	**28.580**	**31.000**	**33.902**
34	**29.916**	**32.682**	**35.925**
35	**31.253**	**34.365**	**37.948**
36	**32.589**	**36.047**	**39.971**
37	**33.925**	**37.729**	**41.994**
38	**35.261**	**39.411**	**44.018**
39	**36.597**	**41.094**	**46.041**
40	**37.933**	**42.776**	**48.064**

irradiance condition. For wind speed calculations (see equation (2.4)) the obtained correction (k_{wind}) reflects the necessary decrease in outdoor temperature, as input to the regression model corresponding to a lower wind speed, to yield an equivalent cooling power as that observed under a higher wind speed conditions).

The derived equations for initial corrections (k_{sol_i}):

$$a_{eq1} \cdot \left(T_{out} + k_{sol\_i}\right) + b_{eq1} = a_{eq2} \cdot T_{out} + b_{eq2} \tag{2.1}$$

$$k_{sol\_i}(eq_2) = \frac{a_{eq2} \cdot T_{out} + b_{eq2} - b_{eq1}}{a_{eq1}} - T_{out} \tag{2.2}$$

$$k_{sol\_i}(eq_3) = \frac{a_{eq3} \cdot T_{out} + b_{eq3} - b_{eq2}}{a_{eq2}} - T_{out} \tag{2.3}$$

$$a_{eq1} \cdot (T_{out} - k_{wind}) + b_{eq1} = a_{eq2} \cdot T_{out} + b_{eq2} \tag{2.4}$$

where:

a- slope coefficient of the function defining the correction of the outdoor temperature due to solar irradiance (or wind speed), [−];
b- y-intercept of the function defining the correction of the outdoor temperature due to solar irradiance (or wind speed), [−];
eq_1 - symbol of the function defining the correction of the outdoor temperature due to solar irradiance for the second selected

Table 9
The initial correction (k_{sol_i}) of outdoor temperature due to solar irradiance for Building A.

	Solar irradiance		
	0-250 W/m^2	250-500 W/m^2	>500 W/m^2
	Mean value: 141.3 W/m^2	Mean value: 358.81 W/m^2	Mean value: 676.20W/m^2
T_{out} [°C]	(eq_1) y = 1.3361x - 15.511	(eq_2) y = 1.6823x - 24.516	(eq_3) y = 2.0232x – 32.864
27		0.256	0.509
28		0.515	0.712
29		0.774	0.914
30		1.034	1.117
31		1.293	1.320
32		1.552	1.522
33		1.811	1.725
34		2.070	1.927
35		2.329	2.130
36		2.588	2.333
37		2.847	2.535
38		3.107	2.738
39		3.366	2.941
40		3.625	3.143

range, i.e., in this case 0–250 W/m^2, [−];

eq_2 - symbol of the function defining the correction of the outdoor temperature due to solar irradiance for the second selected range, i.e., in this case 250-500 W/m^2, [−];

eq_3 - symbol of the function defining the correction of the outdoor temperature due to solar irradiance for the third selected range, i.e., in this case >500 W/m^2, [−];

Calculation example of initial correction due to solar irradiance (k_{sol_i}) for Building A:

$$k_{sol\_i}(eq_2) = \frac{1.6823 \cdot T_{out} - 24.516 + 15.511}{1.3361} - T_{out}$$

$$k_{sol\_i}(eq_3) = \frac{2.0232 \cdot T_{out} - 32.864 + 24.516}{1.6823} - T_{out}$$

The first column for the range of 0-250 W/m^2 is empty, because it is the reference point for the initial adjustment for the range of 250 – 500 W/m^2 (the first column for the initial range of the wind speed correction calculations should also remain empty and be used as a reference).

The next step consisted of determining the final correction values (k_{sol_f}) used to adjust the outdoor temperature based on solar irradiance. Additionally, the mean solar irradiance value was calculated for each defined range namely 0–250 W/m^2 (with a mean solar irradiance of 141.3 W/m^2), 250–500 W/m^2 (with a mean solar irradiance of 358.81 W/m^2) and >500 W/m^2 (with a mean solar irradiance of 676.20 W/m^2). For each temperature, the correction is calculated for the specified mean value of solar irradiance in each range (see equation (3.1)-(3.3) and Table 10). A similar interpolation and calculations, as well as the calculation of the mean wind speed for each range, should be performed for the wind speed correction calculations.

Calculation formulas for determining the final correction due to solar irradiance (k_{sol_f}).

$$k_{sol\_f}(eq_1) = \frac{k_{sol\_i}(eq_2)}{2} \ [^\circ C] \tag{3.1}$$

$$k_{sol\_f}(eq_2) = k_{sol\_i}(eq_2) \ [^\circ C] \tag{3.2}$$

$$k_{sol\_f}(eq_3) = k_{sol\_i}(eq_2) + k_{sol\_i}(eq_3) \ [^\circ C] \tag{3.3}$$

Calculation example for Building A – correction due to solar irradiance:

$$k_{sol\_f}(eq_1)\ (27^\circ C) = \frac{0.256}{2} = 0.128 \ [^\circ C]$$

$$k_{sol\_f}(eq_2)\ (27^\circ C) = 0.256\ [^\circ C]$$

$$k_{sol\_f}\ (eq_3)\ (27^\circ C) = 0.256 + 0.509 = 0.765 \ [^\circ C]$$

Due to the limited dataset, the first solar irradiance range (0–250 W/m^2) was used as a reference interval for the initial correction calculations. Accordingly, an interpolation was performed for the final correction value in the first column ($k_{sol\_f}\ (eq_1)$) by assuming half of the value ($k_{sol\_f}\ (eq_2)$) corresponding to the second range (250–500 W/m^2). The final mean value of solar irradiance (250.05 W/m^2) for the first column ($k_{sol\_f}\ (eq_1)$) was also determined as the average of the mean values 141.3 W/m^2 and 358.81 W/m^2 that were obtained for the 0–250 W/m^2 and 250–500 W/m^2 ranges in the process to calculate the initial correction (Table 9), respectively.

Finally, the mean final correction values for outdoor temperature, accounting for solar irradiance, was determined, as indicated in

Table 10
The final correction value (k_{sol_f}) of the outdoor temperature due to solar irradiance for Building A.

	Mean value of solar irradiance		
T_{out} [°C]	**250.05 W/m^2**	**358.81 W/m^2**	**676.20 W/m^2**
27	0.128	0.256	0.765
28	0.258	0.515	1.227
29	0.387	0.774	1.689
30	0.517	1.034	2.151
31	0.646	1.293	2.612
32	0.776	1.552	3.074
33	0.905	1.811	3.536
34	1.035	2.070	3.998
35	1.165	2.329	4.459
36	1.294	2.588	4.921
37	1.424	2.847	5.383
38	1.553	3.107	5.845
39	1.683	3.366	6.306
40	1.812	3.625	6.768
Mean value	**0.970**	**1.940**	**3.767**

the last row of Table 10.

Using the derived final correction of the outdoor temperature due to solar irradiance (k_{sol_f}), the mean values for each solar irradiance level were calculated, and a scatter plot was created based on these results. For the wind speed correction, the derived final outdoor temperature correction due to wind speed should be calculated in the same way, and the mean value should be determined for each wind speed level. Then, a chart should be created based on the obtained results. The regression equations represent the outdoor temperature correction values due to solar irradiance (Fig. 6) and wind speed
(Fig. 7) for analysed Building A and Building B.

Equation 4.A is the correction for the outdoor temperature due to solar irradiance for building A and it has the following form:

$$T_{insol}^{A\ rev} = 0.0064 \cdot Insol - 0.5071,^{\circ} C \tag{4.A}$$

Equation 4.B is the correction of the outdoor temperature due to solar irradiance for building B and it was derived using the same method as for Building A and is presented in the following form:

$$T_{insol}^{B\ rev} = 0.0028 \cdot Insol - 1.0389,^{\circ} C \tag{4.B}$$

The correction of the outdoor temperature due to the mean wind speed (V_{mean}) for building A (equation 5.A) and Building B (equation 5.B) in the form of the equivalent outdoor temperature ($T_V^{A\,rev}$).

$$T_V^{A\,rev} = 1.1884 \cdot V_{mean} - 1.8148 \tag{5.A}$$

$$T_V^{B\,rev} = 1.0502 \cdot V_{mean} - 1.259\ ^{\circ}C \tag{5.B}$$

The calculated corrections of outdoor temperature in response to solar irradiance and wind speed for Building A and Building B differ from one another. This supports the initial hypothesis that such corrections need to be established separately for each building, as each building may respond differently to external environmental factors. i.e. solar irradiance, due to the unique architectural and

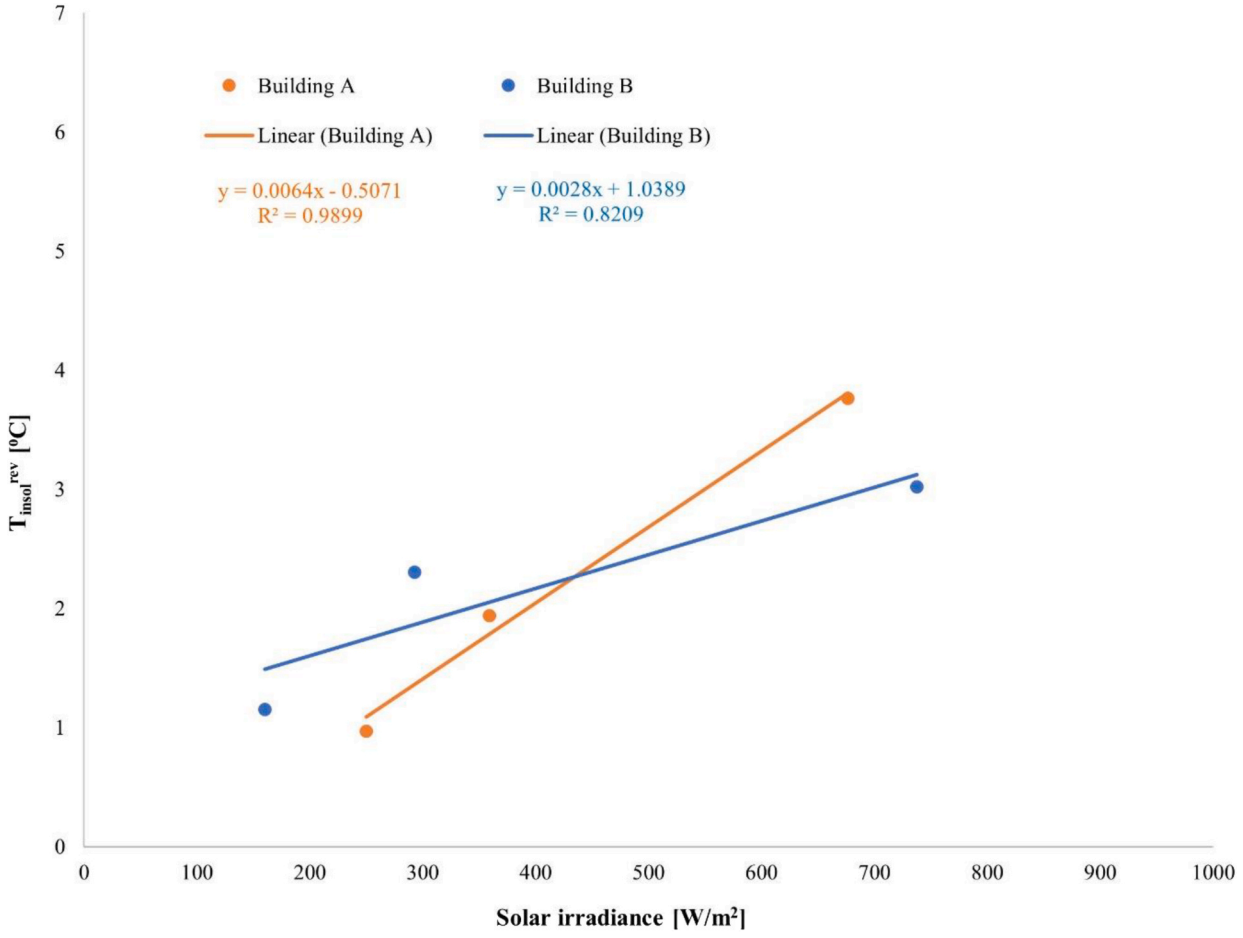

Fig. 6. Equation for correction of the outdoor temperature due to solar irradiance T_{insol}^{REV} for Building A and B.

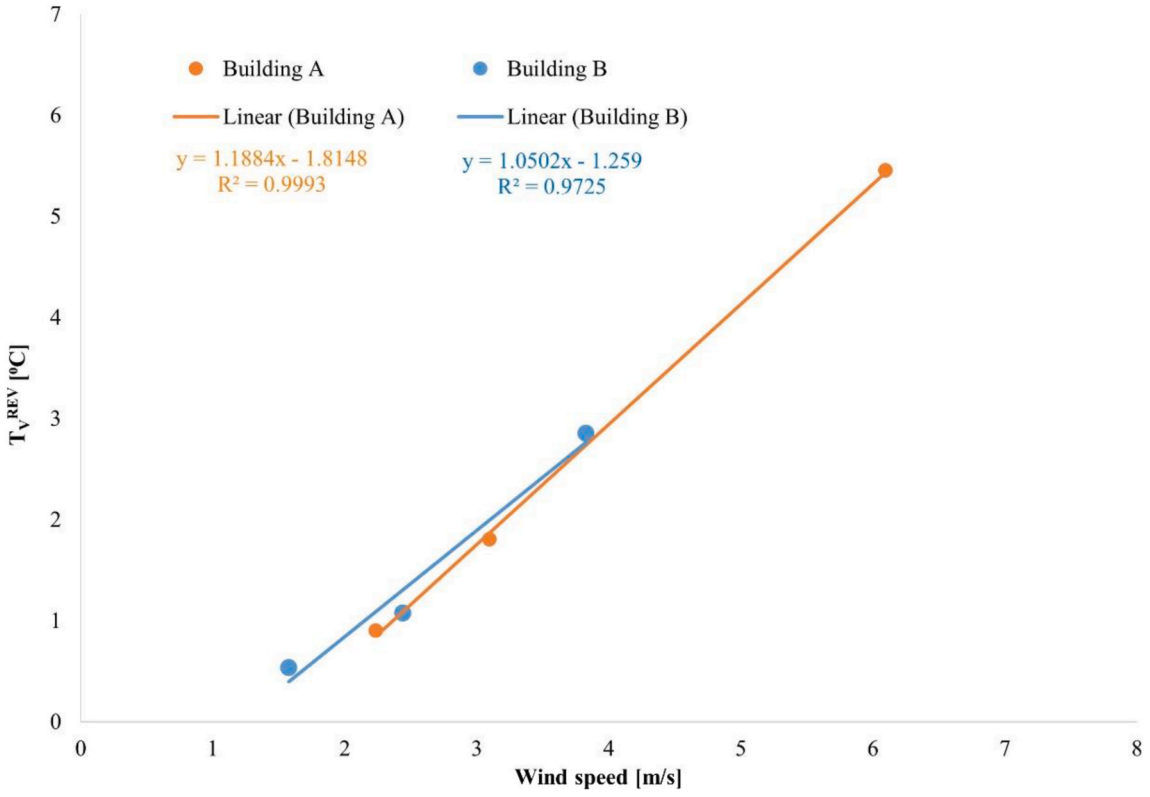

Fig. 7. Equation for correction of the outdoor temperature due to wind speed T_v^{REV} for Building A and B.

system characteristics.

It is acknowledged that the proposed methodology does not explicitly incorporate parameters such as building orientation, window-to-wall ratio, or shading effects when applying the wind speed and solar corrections. However, these influences are indirectly accounted for as part of the resultant effect captured during the process of the correction calculations. Although the developed model includes corrections for outdoor temperature based on physical principles, these corrections are not derived from direct measurements of each building's thermodynamic response under varying environmental conditions. Nevertheless, the combined impact of these factors is inherently embedded in the final energy model. This approach eliminates the need for detailed knowledge of every architectural and design parameter, while still ensuring that the method realistically reflects building-specific thermal responses and significantly speeds up the process of creation of such an energy model.

By collecting hourly data on basic weather parameters, such as outdoor temperature, solar irradiance, and wind speed, it is possible to calculate the equivalent outdoor temperature using the equations provided. This allows for the estimation of the power supplied for air conditioning in specific buildings.

Building A – individual equation for equivalent outdoor temperature:

$$T_{outdoor}{}^{eq} = T_{outdoor} - (1.1884 \cdot V_{mean} - 1.8148) + (0.0064 \cdot I_{nsol} - 0.5071), [^{\circ}C] \quad (6.A)$$

Building B – individual equation for equivalent outdoor temperature:

$$T_{outdoor}{}^{eq} = T_{outdoor} - (1.0502 \cdot V_{mean} - 1.259) + (0.0028 \cdot I_{nsol} + 1.0389), [^{\circ}C] \quad (6.B)$$

In order to evaluate the prediction accuracy, one cooling energy model was developed and validated for each building. **M1** is an energy model that characterises the relationship between cooling energy consumption and the equivalent outdoor temperature for building A (M1_A) and building B (M1_B).

The entire calculation process for determining the building's energy model for cooling in the form of the equivalent outdoor temperature should be carried out individually for each building. The following steps outline the procedure for calculating corrections due to external environmental factors, ensuring accurate and consistent results:

1) A dataset should be constructed for each building by applying boundary conditions to limit the influence of other environmental factors. When calculating corrections, solar irradiance data should be used only for periods with low wind speeds (suggested: below 2.5 m/s), while wind-related data should be considered only for periods with low solar irradiance (suggested: below 250 W/m^2). In

this study, the boundaries were set at 150 W/m^2 for solar irradiance and 1.5 m/s for wind speed. Additionally Table 7 is recommended to guide further dataset construction by filtering.

2) The dataset should be divided into at least three ranges for each factor, using the lowest and highest values to define approximately equal intervals. For each range, a plot of cooling energy consumption versus outdoor temperature should be created, and a linear regression, including the equation and coefficient of determination, should be fitted.
3) Regression plots should be used to calculate cooling energy consumption for each outdoor temperature and range. Results should be summarized in a table, and ranges with logical energy trends should be selected: energy consumption increases with solar irradiance and decreases with wind speed.
4) The initial correction value should be calculated for each outdoor temperature within the selected range using the derived formulas. The first column, representing the first range, should be left empty as a reference.
5) The mean value of the parameter within each range should be calculated. Then the final corrections should be calculated for each outdoor temperature and after mean values of final corrections for each range should be calculated. Due to the limited amount and scope of the data, interpolation of one of the final correction ranges is possible in order to obtain at least three points on the plot showing the relationship between the mean value of the external factor and the mean final correction in each range. A plot of mean final correction values versus the mean external parameter values in each range should be created, and a linear regression should be fitted to derive the general correction formula for the given factor for an individual building.

These energy models enable a thorough analysis of energy consumption patterns, taking into account the influence of the external climate related parameters. The application of corrective adjustments and their comparison is presented in section 4.

4. Results

Equivalent outdoor temperatures have been determined for buildings A and B, taking into account corrections for wind speed and solar irradiance (see section 3). These adjustments allow for more accurate prediction of the actual indoor thermal conditions experienced in the buildings, as both wind speed and solar exposure influence the energy consumption for space cooling.

For Building A, Model 1_A (Fig. 8) that utilises the equivalent outdoor temperature, obtained an R^2 value of 0.6728, representing a solid fit. Due to the polynomial nature of the real data distribution, a third-degree polynomial model was selected for Building A. However, the underlying assumption in model selection is to choose the simplest possible model. Therefore, the model should be selected individually based on the specific characteristics of each building to achieve the best possible model fit.

In the case of Building B, a linear regression model was selected. Model 1_B (Fig. 8), which relies on the dependence of cooling energy consumption on the equivalent outdoor temperature, yielded an R^2 value of 0.6583, pointing to a moderately strong correlation.

The observed differences in cooling energy demand patterns between Poland and Cyprus can be explained by several factors. First, climate plays a key role. In Poland, which has a temperate climate, cooling is mainly limited to periods with very high outdoor temperatures that are rare and sporadic. At low and moderate outdoor temperatures, cooling energy consumption is minimal or zero, and only after exceeding a certain threshold (e.g., 25–27 °C) does it increase rapidly, resulting in an exponential or polynomial relationship. In contrast, in Cyprus, where the climate is hot, cooling demand occurs practically throughout the year and increases more linearly, as an increase of temperature causes a proportional increase in cooling load. Buildings in Cyprus practically operate

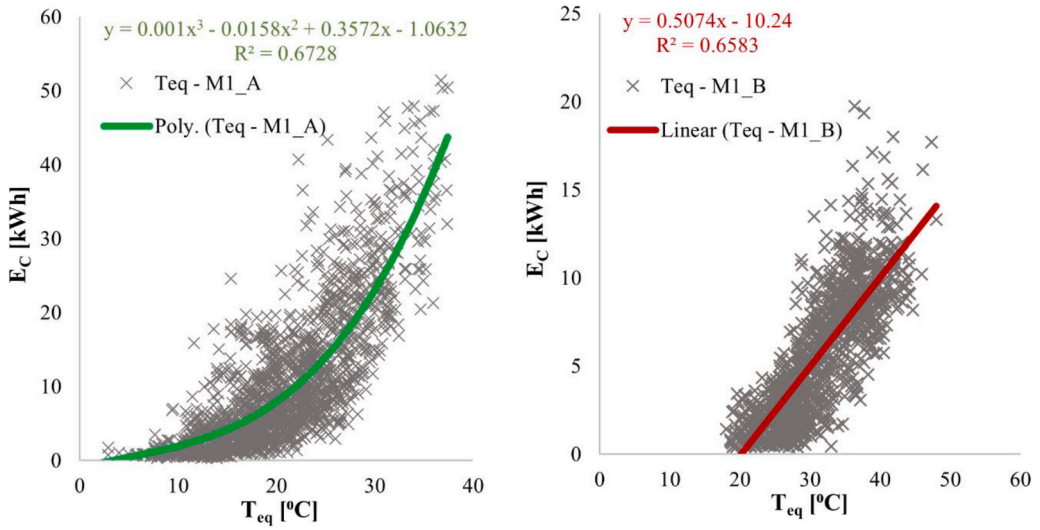

Fig. 8. Hourly cooling energy consumption (E_C) depending on the equivalent outdoor temperature (T_{eq} – M1_A) for Building A and (T_{eq} – M1_B) for Building B.

continuously in cooling mode, without the threshold effect typical of temperate climates. Second, building type and geometry also influence this pattern. Buildings in Poland are often better thermally insulated (designed primarily for heating) to reduce heat losses at low outdoor temperature, while during high outdoor temperature, cumulative heat gains from solar radiation and ambient temperatures sharply increase cooling demand. In Cyprus, thermal insulation limits heat gains, resulting in a linear increase in cooling demand as temperature rises. Finally, cooling system operation further explains this difference. In Poland, air conditioning is often switched on only during peak periods, whereas in Cyprus, cooling systems usually operate continuously, producing continuous, linear behaviour.

Future studies could focus on developing a correction factor related to building thermal inertia or resistance-capacitance (RC) characteristics to improve the accuracy of the method. Incorporating thermal inertia would allow the equivalent temperature to better reflect the dynamic response of the building to outdoor conditions, particularly during periods of rapid outdoor temperature change or solar gain fluctuations. This would enable the model to account for the time lag between outdoor temperature variations and indoor cooling demand, potentially resulting in higher R^2 values and improved prediction accuracy. Therefore, integrating building-specific thermal mass and heat storage effects into the equivalent temperature calculations is recommended as a promising direction for further research.

4.1. Validation

The validation of the derived models was performed using measured data for one month for each building, namely September 2023 for Building A and September 2024 for Building B. This data was not used for the development of the corresponding models. The results for building A are illustrated in Fig. 9 and for building B in Fig. 10.

For the validation period, the errors were calculated based on the cooling energy demand predicted by the developed models, compared to the actual energy consumption for cooling. The calculated errors are presented in Table 11. To ensure more reliable results only data where the outdoor temperature (T_{out}) was greater than 26 °C were selected for validation. The selection of data with T_{out}>26 °C was intentional, as this outdoor temperature range is more relevant for the use of cooling. Temperatures above 26 °C typically indicate conditions where cooling systems are actively used to maintain comfortable indoor environments. By focusing on

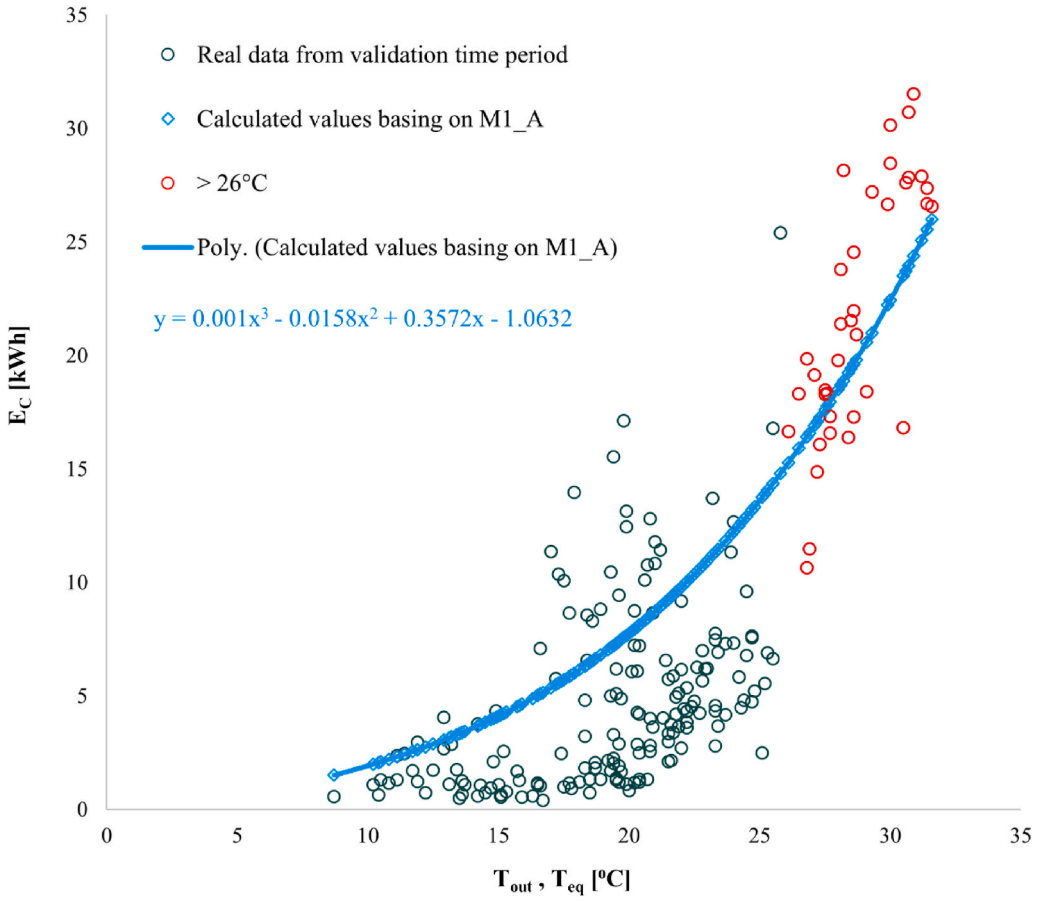

Fig. 9. Comparison of real data from the validation period (September 2023) with the hourly cooling energy consumption (E_C) models for cooling for the equivalent outdoor temperature (T_{eq} – M1_A) for Building A.

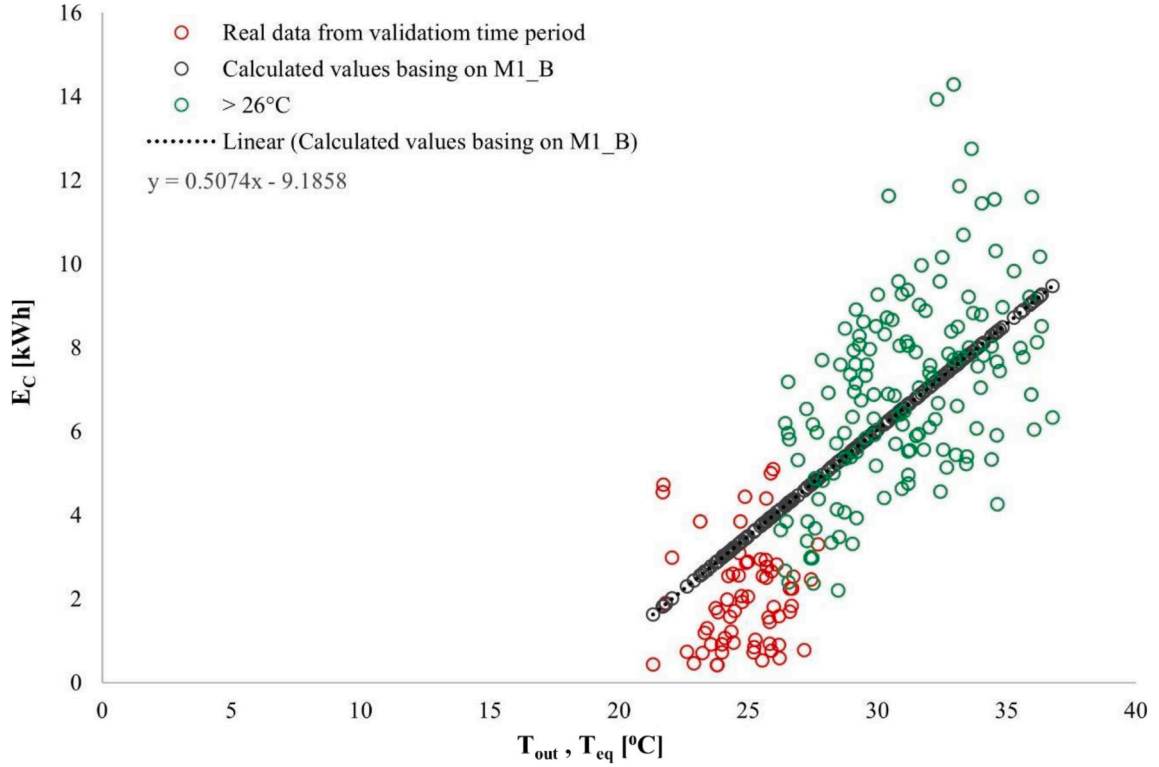

Fig. 10. Comparison of real data from the validation period (September 2024) with the hourly cooling energy consumption (E_C) models for cooling for the equivalent outdoor temperature (T_{eq} – M1_B) for Building B.

Table 11
Statistical indexes comparing the predicted with the measured cooling energy consumption in building A and Building B using developed models and screened data for T_{out} above 26 °C.[a]

Model	Mean MAPE [%]		Mean CVRMSE [%]	
	Building		Building	
	A	B	A	B
T_{eq} (M1_A; M1_B)	**13.15** (127.09)	**17.87** (29.13)	**16.59** (60.91)	**22.36** (33.73)

[a] The values in the parentheses capture the corresponding results from using the entire database without any screening, and the bolded values represent results from using the dataset with T_{out} above 26 °C.

these conditions, the analysis ensures that the data represents realistic and reliable scenarios for the operation of the cooling systems in the two buildings, as it captures the periods when cooling demand is significant.

The results presented in Table 11 indicate that the model accuracy improves significantly when the validation exercise is limited to the periods with outdoor temperatures that exceed 26 °C. When the full dataset was used (values in parenthesis in Table 11), the mean absolute percentage error (MAPE) and the coefficient of variation of the root mean square error (CVRMSE) were noticeably higher for both buildings. Specifically, for Building A. This can be attributed to the fact that Building A is located in a cooler climate zone, where a greater proportion of the recorded temperatures fell below the 26 °C. As a result, the inclusion of low-temperature periods - during which the cooling system was either inactive or at minimal operating conditions - introduces variability that reduces the accuracy of the model fit. These periods do not reliably reflect the building's cooling dynamics and thus distort the model performance evaluation.

In contrast, when only periods with outdoor temperatures above 26 °C were considered, both error metrics decreased substantially. For Building A MAPE of M1_A model decreased to 13.15% and the CVRMSE to 16.59% or Building B M1_B model, CVRMSE dropped to 22.26% and MAPE to 17.87%, suggesting improved alignment between the model predictions and the observed cooling energy consumption.

This pattern suggests that the model more accurately captures the cooling behaviour during periods of consistent system operation, typically associated with higher outdoor temperatures. During cooler periods, the system may operate irregularly or remain inactive, introducing variability that the model cannot fully capture. As a result, including such periods in the validation process inflates error metrics and may misrepresent the model's true performance under cooling load conditions. These findings underscore the importance

of context-specific validation strategies in energy modelling. Applying temperature-based filtering enables a more realistic assessment of model performance, particularly in applications focused on peak demand or warm-season energy planning. Additionally, the intended use of the buildings differs significantly. The operation of the cooling system is much more stable in an office building, where the occupancy schedule is more consistent compared to an educational building. These differences are particularly noticeable during the summer season, which represents the cooling period for buildings. In the case of educational buildings, the absence of students on campus and in university facilities during the summer significantly impacts the operation of the cooling systems. Moreover, this is also a vacation period when many university students and staff members are on vacation leave. The larger the analysed cooled area, and the more stable the building usage schedule is the more reliable the results, as they better reflect how the building behaves under varying conditions.

Figs. 9 and 10 shows a comparison of actual energy consumption data for cooling purposes during the model validation period, i.e., September 2023 (Building A) and September 2024 (Building B), alongside forecasted data based on the two baseline models, M1_A and M1_B. It is clear that the relationship between energy consumption for cooling and equivalent temperature is similar to the previously proposed models, which allows for reliable energy consumption predictions.

A comparison of Figs. 9 and 10 clearly illustrates the climatic differences between the two buildings. In the case of Building A, there are significantly fewer instances of outdoor air temperatures exceeding 26 °C, since the building is located in a cooler climate zone. Despite the limited number of high-temperature data points, the graphical representation also reveals that the deviations from the model's predicted function are generally smaller for Building A compared to Building B. This suggests a more consistent model fit for Building A, potentially due to more stable or predictable system behaviour for higher temperatures under the prevailing climatic conditions.

4.2. ANN analysis and comparison with the proposed method

In order to further evaluate the robustness of the proposed approach, the same dataset was also analysed using artificial neural networks (ANN). This allowed for a direct comparison between the physically based equivalent outdoor temperature method and a data-driven modeling technique. By applying both approaches to identical input data for the creation of building energy models and for the validation of energy models, it was possible to assess not only the predictive accuracy of each method but also their relative advantages and limitations in forecasting cooling energy demand.

For both analysed buildings artificial neural networks of the Multilayer Perceptron (MLP) type were employed to model the cooling energy consumption of two analysed public utility buildings. The input variables were the hourly outdoor temperature, wind speed, and solar radiation intensity values, while the output variable was the cooling energy consumption. For the neural network models, the same datasets as in the proposed in this article method was used - with filtering of the input dataset (basing on data filtering assumptions from Table 6). For validation purposes, data also from the same one full month of September were used. Networks were generated in batch mode with the following configuration: minimum number of hidden neurons = 3, maximum = 10. A total of 20 candidate networks were trained, of which the five best-performing models were retained for further analysis.

The filtered input dataset for Building A was used to retrain a set of multilayer perceptron (MLP) networks with various hidden layer configurations (ranging from 4 to 10 neurons). All networks employed the BFGS training algorithm and the sum-of-squares (SOS) error function, with different activation functions tested in hidden and output layers. Table 12 summarizes the results of the ANN analyses, presenting the quality of fit and error metrics for the retained networks. The networks achieved high training and validation quality, with correlation coefficients ranging between 0.85 and 0.87. It is important to note that the validation quality closely matched the training quality, suggesting robust generalization and the absence of significant overfitting. Training errors varied between 10.55 and 11.87, while validation errors ranged from 13.12 to 14.00, indicating stable predictive accuracy across the retained networks. Among the tested architectures, MLP 3-9-1 (ID 2) demonstrated the best balance, with the highest training quality (0.871) and the lowest training error (10.55), as well as a relatively low validation error (13.12).

The sensitivity analysis (results presented in Table 13) of the filtered dataset for Building A confirmed that outdoor air temperature was the dominant predictor of cooling demand, with a mean sensitivity value of 4.287 °C across the networks. Wind speed and solar radiation both showed substantially lower sensitivity values (≈1.033 m/s and ≈1.031 W/m^2 respectively), indicating that their influence on the model's predictions was comparatively minor. These results are consistent with physical expectations for a temperate climate, where cooling loads are primarily driven by variations in outdoor air temperature rather than solar or convective effects.

Table 14 summarizes the results of the ANN analyses, presenting the quality of fit and error metrics for the retained networks. The neural networks trained on the filtered dataset for Building B also achieved high training quality values, ranging from 0.864 to 0.876, which indicates strong correlation between predicted and actual cooling demand. The validation quality was consistently lower, in the range of 0.764–0.779, but remained stable across the networks, indicating robust generalization to out-of-sample data.

The error values confirmed the robustness of the models. Training errors varied between 1.59 and 1.73, while validation errors ranged from 2.03 to 2.14. The relatively small difference between training and validation errors indicates that overfitting was limited and that the filtering procedure contributed to stabilizing the models' predictive performance.

Among the tested architectures, MLP 3-8-1 (ID 3) achieved the highest training quality (0.876) and the lowest training error (1.59), though at the cost of a slightly higher validation error (2.14). Conversely, MLP 3-7-1 (ID 5) and MLP 3-6-1 (ID 4) offered the lowest validation errors (≈2.03–2.05) with balanced quality values, suggesting that these models generalized slightly better to unseen data.

The sensitivity analysis after data filtering conducted for Building B (Table 15) shows that both outdoor air temperature and solar radiation mostly influence cooling demand predictions, with a mean sensitivity values of 3.793 °C and 1.454 W/m^2, respectively. Wind speed exhibited the lowest contribution, with a mean value of 1.021 m/s, confirming its marginal role compared with thermal and

Table 12
Summary for ANN created for building A – dataset after data filtering.

ID	Network name	Quality (training)	Quality (validation)	Error (training)	Error (validation)	Training algorithm	Error function	Activation (hidden)	Activation (output)
1	MLP 3-10-1	0.863	0.867	11.15	14.00	BFGS 16	SOS	Linear	Logistic
2	MLP 3-9-1	0.871	0.866	10.55	13.12	BFGS 10000	SOS	Tanh	Logistic
3	MLP 3-4-1	0.863	0.867	11.15	14.00	BFGS 16	SOS	Linear	Logistic
4	MLP 3-7-1	0.863	0.867	11.15	14.00	BFGS 16	SOS	Linear	Logistic
5	MLP 3-9-1	0.855	0.872	11.88	13.28	BFGS 17	SOS	Linear	Exponential

Table 13
Sensitivity analysis for Building A – training sample (with data filtering).

Network	Temperature [°C]	Wind Speed [m/s]	Solar Radiation [W/m^2]
1. MLP 3-10-1	4.262	1.025	1.025
2. MLP 3-9-1	4.793	1.071	1.063
3. MLP 3-4-1	4.262	1.025	1.025
4. MLP 3-7-1	4.262	1.025	1.025
5. MLP 3-9-1	3.855	1.019	1.016
Mean value	**4.287**	**1.033**	**1.031**

Table 14
Summary for ANN created for building B – with data filtering.

ID	Network name	Quality (training)	Quality (validation)	Error (training)	Error (validation)	Training algorithm	Error function	Activation (hidden)	Activation (output)
1	MLP 3-8-1	0.871	0.774	1.65	2.08	BFGS 1722	SOS	Exponential	Tanh
2	MLP 3-4-1	0.864	0.769	1.73	2.06	BFGS 777	SOS	Exponential	Tanh
3	MLP 3-8-1	0.876	0.764	1.59	2.14	BFGS 10000	SOS	Logistic	Logistic
4	MLP 3-6-1	0.871	0.775	1.65	2.05	BFGS 10000	SOS	Exponential	Exponential
5	MLP 3-7-1	0.869	0.779	1.67	2.03	BFGS 10000	SOS	Exponential	Tanh

Table 15
Sensitivity analysis for Building B – training sample (with data filtering).

Network	Temperature [°C]	Wind Speed [m/s]	Solar Radiation [W/m^2]
1. MLP 3-8-1	3.776	1.026	1.437
2. MLP 3-4-1	3.544	1.011	1.669
3. MLP 3-8-1	3.945	1.033	1.407
4. MLP 3-6-1	3.827	1.023	1.303
5. MLP 3-7-1	3.871	1.013	1.453
Mean value	**3.793**	**1.021**	**1.454**

radiative drivers.

Compared with the previous analysis for Building A, this analysis (for Building B) highlights a more pronounced influence of solar radiation. While temperature remains the dominant predictor, the relative increase in sensitivity to irradiance reflects the importance of solar gains under Mediterranean climatic conditions.

For both buildings, ANN analyses were also carried out using the raw dataset without filtering according to initial assumptions from Table 6. In addition, the results demonstrated that after applying data filtration the quality of network fitting improved, confirming the validity and importance of the filtering step.

The application of multilayer perceptron (MLP) neural networks to predict building cooling demand demonstrated that such data-driven models are capable of capturing the nonlinear relationships between meteorological inputs and cooling energy use. However, the obtained results indicate that their performance did not substantially exceed that of the proposed equivalent outdoor temperature (T_{eq}) method. Across both case studies, the networks achieved correlation coefficients in the range of 0.87 for training data. For Building A, the coefficient of determination (R^2) remained stable, in some cases even exceeding the training values for the validation dataset, whereas for Building B they decreased from 0.87 to 0.77. This suggests that the models for Building A generalized well to unseen data, while in the case of Building B the drop in R^2 indicates reduced robustness and a potential sensitivity to validation conditions. The error measures confirmed that the neural networks offered a comparable level of precision to the simplified physical model, without delivering a decisive improvement.

This outcome suggests that the advantages of ANN-namely their ability to model complex nonlinear interactions-were limited by the restricted set of input variables. At the same time, the T_{eq} approach, while conceptually simpler, incorporates physical corrections

for solar radiation and wind speed, enabling it to capture the dominant effect of meteorological conditions on cooling demand. As a result, the neural networks did not demonstrate a clear superiority over the T_{eq} method, reinforcing the value of simplified, physically interpretable models in contexts where data availability is limited and model transparency is required.

For each generated neural network, the Mean Absolute Percentage Error (MAPE) and the Coefficient of Variation of the Root Mean Square Error (CVRMSE) were calculated using the validation data. The results refer to the entire analysed dataset (bold values), and the dataset that corresponds to outdoor temperatures above 26 °C (in parentheses). The comparative analysis demonstrates that the Teq-based method consistently yields the lowest errors, both in overall performance and in high-temperature ranges, confirming its superior predictive accuracy compared to the other approaches. A detailed comparison of the error values is presented in Table 16.

4.3. Limitations

This study has certain limitations that should be acknowledged. First, the analysis was conducted on a selected set of buildings, which may restrict the generalization of the results to other building types or operational conditions. In this study, the relationships were examined and formulated for two buildings located in two distinct climate zones. Although the proposed method is universal, it requires individual customization for each building due to the need for building-specific selection of data filtering ranges during the model development phase, as well as the calculation of correction factors to account for local solar irradiance values and wind speed conditions. The presented method was developed with the aim of creating a universal approach for building model generation applicable to various building types and climatic regions. The two case study buildings analysed in this study were selected as representative building types (office and educational) and located in two distinct European locations. However, the method has not yet been tested on a broader range of building types or geographic locations. Second, although the proposed universal method enables the consideration of the various dependencies of cooling energy demand on dynamic weather conditions, the validation was conducted over a limited time period. Third, at this stage, the method does not account for occupant behavior profiles or other internal conditions, which could influence the building's overall energy performance. Moreover, due to the lack of available data, indoor temperature measurements were not included in the analysis. The authors plan to incorporate predicted indoor temperature profiles in future work to enhance the model's accuracy and applicability. Despite these limitations, the findings provide valuable insights into realistic representation of building thermal behavior in case of power demand for cooling and influence of external factors (weather conditions). Future research is recommended to incorporate occupant behavior profiles and/or other internal conditions into the energy model what may improve its accuracy in representing real building energy performance.

5. Conclusions

This study presents a simple and accurate methodology for developing a real energy model of a building and its cooling system that accounts for external conditions, though the influence of occupants is not yet included. The model was validated using high-resolution monitoring data from two buildings and site-specific meteorological variables, such as outdoor temperature, wind speed, and solar irradiance. It is based on an equivalent outdoor temperature (T_{eq}), calculated from hourly data, which adjusts outdoor temperature by accounting corrections due to wind speed and solar irradiance to better represent building thermal behaviour in cooling mode.

Accurate analysis of building cooling energy performance requires datasets that reflect typical system operation. That is why, periods of low or no usage, such as weekends, holidays, and off-hours, were excluded to prevent distortions. By focusing on active operational periods, the study ensures robust correlations between energy consumption and environmental factors, minimizing the impact of unrelated variables and enhancing analytical reliability.

A key step in developing the energy model is the careful selection of the appropriate cooling system operational data and the corresponding meteorological variables to isolate the effect of specific external factors. In this study, the correction for outdoor temperature due to solar irradiance was calculated using data with wind speeds below 1.5 m/s, while the correction for wind speed was calculated using data with solar irradiance below 150 W/m^2, minimizing the influence of other environmental variables on the cooling energy consumption.

In the error calculation process, additional assumptions were introduced to ensure the analysis focused on the conditions under

Table 16
Comparative values of MAPE and CVRMSE for validation data obtained by use of different neural network models and proposed T_{eq} method.[a]

Building	Mean MAPE [%]					
	T_{eq} (M1)	1 MLP	2 MLP	3 MLP	4MLP	5MLP
A	**13.15** (127.09)	**21.22** (156.19)	**20.18** (151.99)	**19.61** (155.17)	**21.43** (153.66)	**24.73** (144.28)
B	**17.87** (29.13)	**31.57** (43.92)	**29.35** (38.36)	**34.89** (47.06)	**29.57** (39.38)	**30.47** (41.76)
Building	**Mean CVRMSE [%]**					
	T_{eq} (M1)	1 MLP	2 MLP	3 MLP	4 MLP	5 MLP
A	**16.59** (60.91)	**20.49** (47.00)	**19.10** (47.14)	**18.94** (46.81)	**20.10** (47.34)	**21.56** (46.88)
B	**22.36** (33.73)	**32.25** (45.46)	**31.61** (46.58)	**27.65** (43.11)	**32.49** (46.03)	**32.62** (46.00)

[a] The values in parentheses capture the corresponding results from using the entire database without any screening, and the bolded values represent results for the dataset with T_{out} above 26 °C.

which air conditioning is utilised most extensively, specifically for outdoor temperatures exceeding 26 °C. Comparing the two analysed prediction methods, T_{eq} and **ANN**, based on the MAPE results, the T_{eq} method demonstrated better performance, showing lower MAPE and higher accuracy than the ANN models. The T_{eq} method achieved the lowest errors for both Building A (13.15%) and Building B (17.87%), outperforming all ANN (MLP) models. The MAPE values for ANN methods increased consistently with the number of layers, indicating a greater bias. Therefore, the T_{eq} approach proved to be more accurate and stable in terms of mean absolute percentage error compared to ANN-based models.

The main conclusions drawn from this study are outlined below:

- A simple, data-driven cooling energy model based on real building measurements was developed, enabling building-specific short-term forecasting without simulations.
- The equivalent outdoor temperature (T_{eq}), including wind speed and solar irradiance corrections, effectively captures external influences on cooling energy consumption.
- Careful selection of operational and meteorological data significantly improves model accuracy and reliability.
- The T_{eq}-based method outperformed ANN models for both buildings, achieving lower MAPE values and greater stability.
- The proposed approach supports forecast-based control of cooling systems and can be extended to include additional climate parameters and occupant influence.

The proposed method is based on physical data from real buildings rather than simulations, enabling a simple, building-specific approach and supporting forecast-based control of cooling systems. Developing predictive models for cooling is more complex than for heating. As noted by Cholewa et al. [39] [41] [42], heating models based on equivalent temperature require no data filtering due to the stable thermal behaviour of buildings in the heating season. In contrast, cooling demand is highly dynamic and influenced by solar radiation, internal gains, occupancy, and ventilation, requiring careful selection of operational data in order to properly capture external influences on cooling energy consumption. The method can be further extended to include other climate parameters, such as humidity, and latent cooling loads, which may influence the cooling load of a specific cooling system that will improve accuracy.

Future research will extend the method to a larger number of buildings across diverse climate zones and incorporate the interactions between occupants and cooling energy consumption. This will enhance the building energy model, currently based on external factors, by including internal factors such as occupant behaviour, enabling more accurate short-term forecasting of cooling demand without extensive simulations. Additionally, the suitability of the method for different building types can be evaluated by comparing its results with predictions from energy simulation models or similar approaches. Finally, future work will include the application of the proposed method in forecast control of cooling systems.

CRediT authorship contribution statement

Wiktoria Łokczewska: Writing – review & editing, Writing – original draft, Resources, Methodology, Investigation, Formal analysis, Conceptualization. **Tomasz Cholewa:** Writing – review & editing, Writing – original draft, Supervision, Methodology, Investigation, Conceptualization. **Amelia Staszowska:** Writing – review & editing, Writing – original draft, Supervision. **Constantinos A. Balaras:** Writing – review & editing, Writing – original draft. **Paris A. Fokaides:** Writing – review & editing. **Chirag Deb:** Writing – review & editing. **Gerardo Maria Mauro:** Writing – review & editing. **Fabrizio Ascione:** Writing – review & editing.

Declaration of competing interest

The authors declare that they have no known competing financial interests or personal relationships that could have appeared to influence the work reported in this paper.

Acknowledgments

This study was supported by NAWA STER Programme Internationalization of Lublin University of Technology Doctoral School II - IDeaS of LUT II.

Data availability

Data will be made available on request.

References

[1] IEA, Energy Efficiency 2024, IEA, Paris, 2024. https://www.iea.org/reports/energy-efficiency-2024Licence:CCBY4.0. (Accessed 26 September 2025).
[2] International Energy Agency, Tracking Clean Energy Progress 2023, IEA, Paris, France, 2023. https://www.iea.org/reports/tracking-clean-energy-progress-2023. (Accessed 26 September 2025).
[3] United Nations Environment Programme, Global Status Report for Buildings and Construction: Beyond Foundations: Mainstreaming Sustainable Solutions to Cut Emissions from the Buildings Sector, 2024. Nairobi.
[4] IEA, Keeping Cool in a Hotter World is Using More Energy, Making Efficiency More Important than Ever, IEA, Paris, 2023. https://www.iea.org/commentaries/keeping-cool-in-a-hotter-world-is-using-more-energy-making-efficiency-more-important-than-ever. (Accessed 26 September 2025). Licence: CC BY 4.0.

[5] IEA, The Future of Cooling, IEA, Paris, 2018. https://www.iea.org/reports/the-future-of-cooling. (Accessed 26 September 2025). Licence: CC BY 4.0.
[6] Independent Statistics and Analysis, U.S. Energy Information Administration, Annual Energy Outlook, AEO2023.
[7] D.P. van Vuuren, J. Edmonds, M. Kainuma, et al., The representative concentration pathways: an overview, Clim. Change 109 (2011) 5, https://doi.org/10.1007/s10584-011-0148-z.
[8] United Nations Environment Programme, & Global alliance for buildings and construction (2025). Not just another brick in the wall: the solutions exist - scaling them will build on progress and cut emissions fast. Global Status Report Build. Construct. 2024/2025. https://wedocs.unep.org/20.500.11822/47214 (access date: 26.September.2025).
[9] IEA, World Energy Outlook 2024, IEA, Paris, 2024. https://www.iea.org/reports/world-energy-outlook-2024. (Accessed 26 September 2025). Licence: CC BY 4.0 (report); CC BY NC SA 4.0 (Annex A).
[10] M. Borowski, K. Zwolińska, Prediction of cooling energy consumption in hotel building using machine learning techniques, Energies 13 (2020) 6226, https://doi.org/10.3390/en13236226.
[11] M. Borowski, K. Zwolińska, Prediction of cooling energy consumption using a neural network on the example of the hotel building, Proceedings 58 (2020) 21, https://doi.org/10.3390/WEF-06917.
[12] Y. Feng, Q. Duan, X. Chen, S.S. Yakkali, J. Wang, Space cooling energy usage prediction based on utility data for residential buildings using machine learning methods, Appl. Energy 291 (2021) 116814, https://doi.org/10.1016/j.apenergy.2021.116814. ISSN 0306-2619.
[13] K. Amasyali, N. El-Gohary, Machine learning for occupant-behavior-sensitive cooling energy consumption prediction in office buildings, Renew. Sustain. Energy Rev. 142 (2021) 110714, https://doi.org/10.1016/j.rser.2021.110714. ISSN 1364-0321.
[14] Y. Feng, Y. Huang, H. Shang, J. Lou, A.D. Knefaty, J. Yao, R. Zheng, Prediction of hourly air-conditioning energy consumption in office buildings based on gaussian process regression, Energies 15 (2022) 4626, https://doi.org/10.3390/en15134626.
[15] M. Khorrami, B, A. Soleimani, A. Pinnarelli, et al., Forecasting heating and cooling loads in residential buildings using machine learning: a comparative study of techniques and influential indicators, Asian J Civ Eng 25 (2024) 1163–1177, https://doi.org/10.1007/s42107-023-00834-8.
[16] X. Zhou, N. Wang, J. Zou, G. Liu, X. Zhuang, G. Liu, Analysis and prediction of energy consumption in office buildings with variable refrigerant flow systems: a case study, J. Build. Eng. 97 (2024) 110936, https://doi.org/10.1016/j.jobe.2024.110936. ISSN 2352-7102.
[17] F. Ascione, R.F. De Masi, V. Festa, G.M. Mauro, G.P. Vanoli, Optimizing space cooling of a nearly zero energy building via model predictive control: energy cost vs comfort, Energy Build. 278 (2023) 112664, https://doi.org/10.1016/j.enbuild.2022.112664. ISSN 0378-7788.
[18] B. Yue, Z. Wei, C. Zheng, Y. Ding, B. Li, D. Li, X. Liang, X. Zhai, Power consumption prediction of variable refrigerant flow system through data-physics hybrid approach: an online prediction test in office building, Energy 278 (Part A) (2023) 127826, https://doi.org/10.1016/j.energy.2023.127826. ISSN 0360-5442.
[19] L. Li, X. Su, X. Bi, Y. Lu, X. Sun, A novel Transformer-based network forecasting method for building cooling loads, Energy Build. 296 (2023) 113409, https://doi.org/10.1016/j.enbuild.2023.113409. ISSN 0378-7788.
[20] C. Lu, S. Li, S.R. Penaka, T. Olofsson, Automated machine learning-based framework of heating and cooling load prediction for quick residential building design, Energy 274 (2023) 127334, https://doi.org/10.1016/j.energy.2023.127334. ISSN 0360-5442.
[21] Y. Zhao, W. Li, J. Zhang, C. Jiang, S. Chen, Real-time energy consumption prediction method for air-conditioning system based on long short-term memory neural network, Energy Build. 298 (2023) 113527, https://doi.org/10.1016/j.enbuild.2023.113527. ISSN 0378-7788.
[22] B. Chen, W. Yang, B. Yan, K. Zhang, An advanced airport terminal cooling load forecasting model integrating SSA and CNN-transformer, Energy Build. 309 (2024) 114000, https://doi.org/10.1016/j.enbuild.2024.114000. ISSN 0378-7788.
[23] R. Vergés, K. Gaspar, N. Forcada, Predictive modelling of cooling consumption in nursing homes using artificial neural networks: implications for energy efficiency and thermal comfort, Energy Rep. 12 (2024) 2356–2372, https://doi.org/10.1016/j.egyr.2024.08.029. ISSN 2352-4847.
[24] X. Huang, Y. Han, J. Yan, X. Zhou, Hybrid forecasting model of building cooling load based on EMD-LSTM-Markov algorithm, Energy Build. 321 (2024) 114670, https://doi.org/10.1016/j.enbuild.2024.114670. ISSN 0378-7788.
[25] C. Song, H. Yang, X.B. Meng, P. Yang, J. Cai, H. Bao, K. Xu, A novel deep-learning framework for short-term prediction of cooling load in public buildings, J. Clean. Prod. 434 (2024) 139796, https://doi.org/10.1016/j.jclepro.2023.139796. ISSN 0959-6526.
[26] C. Park, I. Kim, W. Kim, Transfer learning–based energy consumption prediction for variable refrigerant flow system in buildings, Appl. Therm. Eng. 267 (2025) 125811, https://doi.org/10.1016/j.applthermaleng.2025.125811. ISSN 1359-4311.
[27] G. Aruta, F. Ascione, N. Bianco, G.M. Mauro, F. Villano, Artificial neural networks to forecast building heating/cooling demand and climate resilience based on envelope parameters and new climatic stress indices, J. Build. Eng. 108 (2025) 112849, https://doi.org/10.1016/j.jobe.2025.112849. ISSN 2352-7102.
[28] P.C. Hsu, L. Gao, Y. Hwang, Comparative study of LSTM and ANN models for power consumption prediction of variable refrigerant flow (VRF) systems in buildings, Int. J. Refrig. 169 (2025) 55–68. ISSN 0140-7007.
[29] Q. Gue, Z. Tian, Y. Ding, N. Zhu, An improved office building cooling load prediction model based on multivariable linear regression, Energy Build. 107 (2015) 445–455, https://doi.org/10.1016/j.enbuild.2015.08.041. ISSN 0378-7788.
[30] S. Chen, X. Zhou, G. Zhou, C. Fan, P. Ding, Q. Chen, An online physical-based multiple linear regression model for building's hourly cooling load prediction, Energy Build. 254 (2022) 111574, https://doi.org/10.1016/j.enbuild.2021.111574. ISSN 0378-7788.
[31] C. Fan, Y. Ding, Cooling load prediction and optimal operation of HVAC systems using a multiple nonlinear regression model, Energy Build. 197 (2019) 7–17, https://doi.org/10.1016/j.enbuild.2019.05.043. ISSN 0378-7788.
[32] C. Zhang, Y. Zhao, X. Zhang, C. Fan, T. Li, An improved cooling load prediction method for buildings with the estimation of prediction intervals, Procedia Eng. 205 (2017) 2422–2428, https://doi.org/10.1016/j.proeng.2017.09.967. ISSN 1877-7058.
[33] X. Lin, Z. Tian, Y. Lu, H. Zhang, J. Niu, Short-term forecast model of cooling load using load component disaggregation, Appl. Therm. Eng. 157 (2019) 113630, https://doi.org/10.1016/j.applthermaleng.2019.04.040. ISSN 1359-4311.
[34] C. Fan, F. Xiao, Y. Zhao, A short-term building cooling load prediction method using deep learning algorithms, Appl. Energy 195 (2017) 222–233, https://doi.org/10.1016/j.apenergy.2017.03.064. ISSN 0306-2619.
[35] H. Yu, F. Zhong, Y. Du, X. Xie, Y. Wang, X. Zhang, S. Huang, Short-term cooling and heating loads forecasting of building district energy system based on data-driven models, Energy Build. 298 (2023) 113513, https://doi.org/10.1016/j.enbuild.2023.113513. ISSN 0378-7788.
[36] C. Feng, C. Zhang, J. Lu, Y. Zhao, Hybrid data-driven and physics-based fast building cooling demand modeling method for large-scale building demand response control, J. Build. Eng. 100 (2025) 111808, https://doi.org/10.1016/j.jobe.2025.111808. ISSN 2352-7102.
[37] A. Jay, K. Campagna, A. Pacquaut, S. Juricic, A. Challansonnex, Extending the validity of co-heating tests to warmer and sunnier weather conditions using an equivalent exterior temperature, Energy Build. 319 (2024) 114483, https://doi.org/10.1016/j.enbuild.2024.114483. ISSN 0378-7788.
[38] I. Omar, A.M. Mohsen, K.A. Hammoodi, H.A. Al-Asadi, Using total equivalent temperature difference approach to estimate air conditioning cooling load in buildings, Journal of Engineering and Thermal Sciences 2 (1) (2022) 59–68, https://doi.org/10.21595/jets.2022.22684.
[39] T. Cholewa, A. Siuta-Olcha, A. Smolarz, P. Muryjas, P. Wolszczak, R. Anasiewicz, C.A. Balaras, A simple building energy model in form of an equivalent outdoor temperature, Energy Build. 236 (2021) 110766, https://doi.org/10.1016/j.enbuild.2021.110766. ISSN 0378-7788.
[40] P. Höppe, The physiological equivalent temperature – a universal index for the biometeorological assessment of the thermal environment, Int. J. Biometeorol. 43 (1999) 71–75, https://doi.org/10.1007/s004840050118.
[41] T. Cholewa, A. Siuta-Olcha, A. Smolarz, P. Muryjas, P. Wolszczak, Ł. Guz, C.A. Balaras, On the short term forecasting of heat power for heating of building, J. Clean. Prod. 307 (2021) 127232, https://doi.org/10.1016/j.jclepro.2021.127232.
[42] T. Cholewa, A. Siuta-Olcha, A. Smolarz, P. Muryjas, P. Wolszczak, Ł. Guz, M. Bocian, C.A. Balaras, An easy and widely applicable forecast control for heating systems in existing and new buildings: first field experiences, J. Clean. Prod. 352 (2022) 131605, https://doi.org/10.1016/j.jclepro.2022.131605.
[43] Eurostat, "Heating and Cooling Degree Days (HDD and CDD)" european commission (access date), https://ec.europa.eu/eurostat/databrowser/view/nrg_chdd_a/default/table. (Accessed 25 January 2026).